POLYMER BRUSH COATED IRON OXIDE NANOPARTICLES FOR BIOMEDICAL APPLICATIONS

by

Mustafa Görkem Bilgin

B.S., Chemistry, Boğaziçi University, 2017

Submitted to the Institute for Graduate Studies in
Science and Engineering in partial fulfillment of
the requirements for the degree of
Master of Science

Graduate Program in Chemistry

Boğaziçi University

2019

Dedicated to my mother and father

ACKNOWLEDGEMENTS

First of all, I would like to thank my thesis supervisor Prof. Dr. Amitav Sanyal since he accepted me as his master student and he gave me a great chance for a research experience in Belgium. Throughout the thesis, his endless support, positive attitudes and trust forced me to work in my projects with passion. I feel very lucky to work under his supervision and I am so thankful for the contributions both in theoretical and experimental chemistry and self-confidence in my personal life.

I would like to thank Prof. Dr. Rana Sanyal for being a role model in my life and her contributions in my research.

I wish to extend my thanks to Assist. Prof. Tuğçe Nihal Gevrek Civan for reviewing and improving my thesis. I am thankful that she was my defense jury.

I am so glad to work with encouraging friends. First of all, I would like to thank Yavuz Öz for his friendship, great support and patience during my research. I want to thank Nora and Filiz for their kind supports in every aspect of my life. I would like to thank the rest of my friends in Sanyal Lab and my ex-lab mate Dr. Laura Chambre for her friendship and being a role model in my life.

I would like to thank my family for their endless love and support.

Finally, I would like to thank The Scientific and Technological Research Council of Turkey (TÜBİTAK) for funding the research (Project No: 217Z072).

ABSTRACT

POLYMER BRUSH COATED IRON OXIDE NANOPARTICLES FOR BIOMEDICAL APPLICATIONS

In recent years, the use of iron oxide nanoparticles has gained importance for biological applications such as hyperthermia, targeted drug delivery, drug release, bio-separation, bio-imaging etc. since they are mono-disperse, biocompatible and more importantly they have magnetic properties. In this thesis, water dispersible, monodisperse, disulfide-containing thiol reactive iron oxide nanoparticles have been synthesized. The disulfide groups were introduced either close to nanoparticle surface or on the exterior of the polymeric coating. Additionally, for surface functionalized polymer brush coated nanoparticles, NHS activated carboxylic acid functionalized were also introduced to enable non-cleavable functionalization using molecules containing amine groups. For the synthesis of such functional molecules, chain transfer agent with/without disulfide bond that is used for RAFT polymerization was modified with catechol anchoring group. These compounds were immobilized onto oleic acid stabilized iron oxide nanoparticles via ligand-exchange reaction. PEG based polymers were grafted from the surface of iron oxide nanoparticles by RAFT polymerization in order to make them water dispersible. The end groups of these polymers are trithiocarbanate groups, which can be modified by azo initiators by radical exchange reactions. For this reason, NHS activated carboxylic acid and disulfide functionalized azo initiators were synthesized and used for the functionalization of grafted polymers. After functionalization of polymer-coated iron oxide nanoparticles, they were able to react with thiol and amine bearing molecules. By using the same chemistry methods, disulfide bearing chain transfer agents were immobilized onto the nanoparticles and PEG based polymers were grown from the surface of nanoparticles by RAFT polymerization and grafting-from approach. Disulfide bearing polymers were cleaved from oxide nanoparticles by using reducing agents. Additionally, this method provides an excellent way to measure the molecular weights of the polymers that are grown by grafting-from approach.

ÖZET

BİYOMEDİKAL UYGULAMALAR İÇİN POLİMER FIRÇA KAPLI DEMİR OKSİT NANOPARÇACIKLAR

Son yıllarda, tek dağılımlı, biyo uyumlu ve daha önemlisi manyetik özelliklere sahip olmalarından dolayı, yüksek ateş, hedefli ilaç dağıtımı ve salınımı, biyo ayırma ve görüntüleme gibi biyolojik uygulamalarda demir oksit kullanımı önem kazanmıştır. Bu tezde, tek dağılımlı ve suda dağılabilir, tiyollere karşı reaktif disülfür bağı içeren demir oksit nanoparçacıklar sentezlenmiştir. Disülfür bağı hem nanoparçacıklara yakın hem de polimer kaplamalarının dışına tanımlanmıştır. Ek olarak, yüzeyleri fonksiyonelleştirilmiş polimer kaplı nanoparçacıklar için, amin içeren moleküller kullanarak, kırılmayan fonksiyonelleştirmeyi mümkün kılmak için NHS ile active edilmiş karboksilli asit grupları da tanıtıldı. Bu molekülleri sentezlemek için, tersinir katılma-ayrışma zincir transfer polimerizasyonunda kullanılacak olan disülfür bağı içeren ve içermeyen zincir transfer ajanı katekol ankraj grubu ile modifiye edilmiştir. Bu moleküllerin ligand değişim reaksiyonu ile oleik asit kaplı demir oksit nanoparçacıkları üzerine immobilizasyonu yapılmıştır. Bu molekülleri suda dağılımlı yapmak için, PEG bazlı polimerler demir oksit nanoparçacıklarının yüzeyi üzerinden tersinir katılma-ayrışma zincir transfer polimerleşmesi ile büyütülmüştür. Bu polimerlerin uçları radikal değişim reaksiyonu ve azo başlatıcılarla modifiye edilebilen tritiokarbonat gruplarıdır. Bu nedenle, N-hidroksisüksinimid ile aktifleştirilmiş karboksilli asit ve disülfür içeren azo başlatıcılar sentezlendi ve bu yüzeyden büyütülen polimerlerlerin fonksiyonelleştirilmesinde kullanıldı. Polimer-kaplı demir oksitlerin fonksiyonelleştirilmesinden sonra, amin ve tiyol içeren bileşiklerle reaksiyona girebildiler. Aynı kimyasal yöntemler kullanılarak, disülfür bağı içeren zincir transfer ajanlarının demir oksit nanoparçacıkları üzerine immobilizasyonu yapıldı ve PEG bazlı polimerler tersinir katılma-ayrışma zincir transfer polimerleşmesi ve yüzeyden büyütme yöntemi ile büyütülmüştür. Disülfür bağı içeren polimerler indirgen maddelerle demir oksit yüzeyinden ayrılmışlardır. Bu yöntem yüzeyden büyütme yöntemi ile büyütülen polimerlerin moleküler ağırlıklarını ölçmek için çok iyi bir yoldur.

TABLE OF CONTENTS

LIST OF FIGURES

LIST OF TABLES

LIST OF ACRONYMS/ ABBREVIATIONS

AcOH	Acetic Acid
ACVA	4’4-Azobis(4-cyanovaleric acid)
AIBN	2,2’-azobisisobutyronitrile
BODIPY	4,4-difluoro-4-bora-3a,4a-diaza-s-indacene
CTA	Chain Transfer Agent
DCC	N,N'-Dicyclohexylcarbodiimide
DCM	Dichloromethane
DLS	Dynamic Light Scattering
DMAP	4-Dimethylaminopyridine
DMF	Dimethylformamide
Dopa	Dopamine
DSC	Disuccinimidyl carbonate
DTT	Dithiothreitol
EDCI	1-Ethyl-3-(3-dimethylaminopropyl)carbodiimide
EtOAc	Ethyl Acetate
FT-IR	Fourier-transform infrared
GPC	Gel Permeation Chromatography
GSH	Glutathione
kDa	Kilodalton
MeOH	Methanol
NHS	N-Hydroxysuccinimide

NMR	Nuclear Magnetic Resonance
OA	Oleic Acid
PDI	Polydispersity Index
PdS	Pyridyl disulfide
PEG	Poly(ethylene glycol)
PEGMEMA	Poly(ethylene glycol) methyl ether methacrylate
RAFT	Reversible Addition Fragmentation Chain Transfer
rt	Room Temperature
TEA	Triethyl Amine
TEM	Transmission Electron Microscopy
THF	Tetrahydrofuran
UV	Ultra-Violet

1. INTRODUCTION

1.1. Iron Oxide Nanoparticles

In recent years, the use of iron oxide nanoparticles has dramatically increased since they can be used in many biological applications such as magnetic resonance imaging (MRI), [1] targeted drug delivery systems, [2] drug release, [3] hyperthermia, [4] and bio-separation. [5] Iron oxide nanoparticles are effective in such areas because they can be obtained with high mono-dispersity in diameters smaller than 100 nm, and are magnetically manipulable. [6] Additionally, they are biocompatible, meaning that they are not harmful to for *in-vivo* applications. They can be obtained with high mono-dispersity, which means that their sizes are similar to one another. Because of this control over size they exhibit narrow and well-defined physical and chemical characteristics. In addition to these properties, iron oxide nanoparticles are also superparamagnetic which means that they can be attracted by a magnet. [7] When a magnetic field is applied to them, they can be guided to a desired place. This property makes them very unique materials for many biomedical applications.

Surface coating of iron oxide nanoparticles plays a quite important role. An appropriate surface coating gives them a high colloidal stability, which prevents their cores from aggregation. Another importance of the surface coating is that they can impart functional aspects required for a desired application, such as favorable biological interactions. [8] Iron oxide nanoparticles can easily come together and agglomerate. Hence they are usually coated with hydrophobic compounds when they are synthesized in organic solvents. In general, well-defined near mono-disperse magnetic nanoparticles are obtained through synthetic approaches in organic solvents. These methodologies yield magnetic nanoparticles that are coated with a monolayer of organic ligands. Unfortunately, these approaches yield magnetic nanoparticles that are not dispersible in water. However, a hydrophilic surface coating is a crucial requirement for their utilization in biological applications. Various approaches including coating with hydrophilic polymers have been

applied to make the organic ligand coated nanoparticles water dispersible to enable biological applications. [9]

1.1.1. Types of Iron Oxide Nanoparticles

There are several types of magnetic nanoparticles such as iron, cobalt and nickel oxides. However, nickel and cobalt oxide magnetic nanoparticles are not suitable for biomedical applications since they are toxic. In contrast, iron oxide nanoparticles can be used in for clinical purposes since they minimal toxicity. Iron oxide nanoparticles can be found in nature as magnetite (Fe_3O_4) or maghemite (γ-Fe_2O_3). The magnetic property of magnetite is higher than that of maghemite. γ-Fe_2O_3 undergoes easier oxidation compared to Fe_3O_4. When γ-Fe_2O_3 gets oxidized while it is in the body, it would create some problems that can affect adversely.[10]

1.1.2. Synthesis of Iron Oxide Nanoparticles

There are several methods to synthesize iron oxide nanoparticles. These synthetic methods are co-precipitation, [11] thermal decomposition, [12] sol-gel, [13] hydrothermal reaction, [14] and microemolsions. [15]

Co-precipitation method is used to synthesize iron oxide nanoparticles in a large scale. Salts of iron are co-precipitated for this purpose. [16] Two types of iron oxide nanoparticles can be synthesized by using this technique. The reaction schemes are shown below: [17]

$$Fe^{2+} + 2Fe^{3+} + 8OH^- \longrightarrow Fe_3O_4 + 4H_2O$$

$$Fe_3O_4 + 2H^+ \longrightarrow Fe_2O_3 + Fe^{2+} + H_2O$$

The other way to synthesize iron oxide nanoparticles is sol-gel method. This process is also known as wet chemical method. It consists of a few steps to reach iron oxide nanoparticles, which involve hydrolysis, condensation and drying. [18]

Hydrothermal synthesis of iron oxides is performed in aqueous environment under high pressure and temperature. Hydrolysis and oxidation are the main pathways in this type of reaction.[19] In this reaction, time, concentration of the reaction medium, temperature are the important parameters that affect the size of the nanoparticles. The increase in amount of water and longer reaction times generally lead to larger iron oxide nanoparticles. [20]

Another way to synthesize iron oxide nanoparticles is using micro-emulsion. It has been reported that micro-emulsion method provides a convenient reaction environment for iron oxide nanoparticles to be synthesized in smaller sizes, with narrow polydispersity. The main components of this method are surfactants, oil and water as reaction medium. [21]

The last way of synthesizing iron oxide nanoparticles is thermal decomposition method. This method is the most widely used among the other methods, since both size and the shape of the nanoparticles can be controlled in a good manner. This synthetic approach furnishes nanoparticles that are near mono-disperse i.e. their sizes are similar to each other. As a result, they show well-defined physical and chemical properties. [22] By using this method, high quality iron oxides nanoparticles can be obtained. [23] This technique involves decomposition of organometallic precursors such as an iron oleate complex in the presence of surfactants and high boiling solvents (Figure 1.1). The iron oleate complex can be synthesized using salts of iron such as $FeCl_3.H_2O$. The salt is mixed with sodium oleate in a solvent mixture including water, ethanol and hexane. The mixture is heated and refluxed for 4 hours to obtain iron oleate complex. [24] In the presence of iron oleate complex, a surfactant such as oleic acid is mixed with a high-boiling solvent such as 1-octadecene. The mixture is heated up to approximately 300 °C under nitrogen protection. Spherical iron oxide nanoparticles with narrow polydispersity and controlled size can be synthesized using this approach. [25]

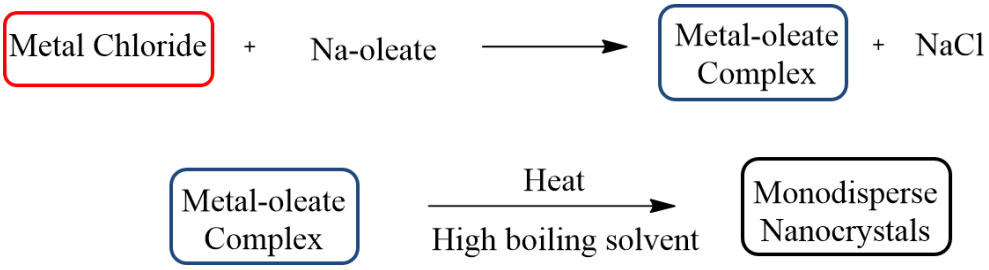

Figure 1.1. Synthetic pathway of thermal decomposition method. [26]

The sizes and the physical appearance of iron oxide nanoparticles can be changed by concentration of reagents, type of solvents, reaction time and temperature (Figure 1.2). More concentrated reactions lead to iron oxide nanoparticles with bigger sizes. [27]

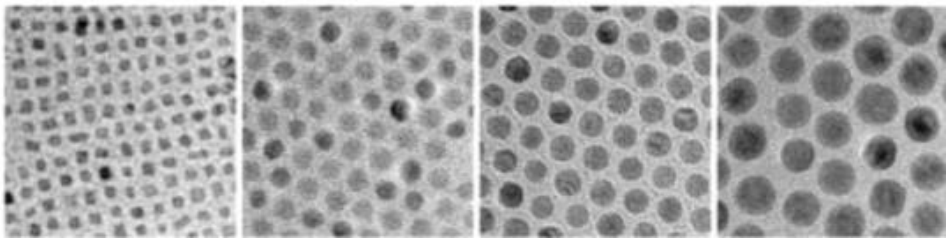

Figure 1.2. TEM images of iron oxide nanoparticles with different sizes (5, 9, 12 and 16 nm, respectively). [28]

1.2. Hydrophobic Coating of Iron Oxide Nanoparticles

Once iron oxide nanoparticles are synthesized, their surfaces need to be coated by surfactants to eliminate the agglomeration which causes an increase in their size and lead to increased polydispersity. Since they have magnetic properties, they tend to stick to one another and aggregate.

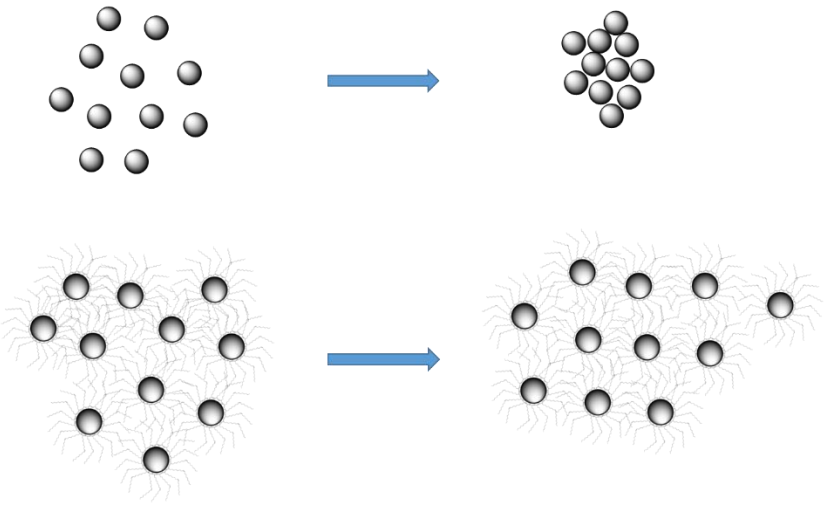

Figure 1.3. Aggregation of uncoated iron oxide nanoparticles with time (top) and prevention of aggregation by hydrophobic coating (bottom).

In order to deactivate this agglomeration, they are coated by hydrophobic surfactants during their synthesis. Thus synthesized organic ligand coated nanoparticles are therefore stable in nonpolar solvents such as chloroform or hexane since the coating materials have long alkyl chains. The surfactants also possess a polar group for attachment onto the surface of iron oxide nanoparticles. For coating purposes, oleic acid is generally used since it has both long alkyl chain and a polar carboxylic acid group. The use of oleic acid as a surfactant, helps to generate monodisperse iron oxide nanoparticles when they are synthesized by thermal decomposition method. [29] Wu et al. proved that oleic acid binds to metal nanoparticles with its carboxylic acid groups and the remaining alkyl groups prevent other nanoparticles from coming and sticking. [30]

1.3. Anchoring Groups Used in Attaching Protecting Groups

An anchoring group is needed for the attachment of the protecting organic ligands groups onto the inorganic nanoparticle surface. For magnetic nanoparticles, these anchoring groups can be a carboxylic acid, [31] a phophonic acid, [32] a trimethoxy silane, [33] and a catechol group shown in Figure 1.4. [34]

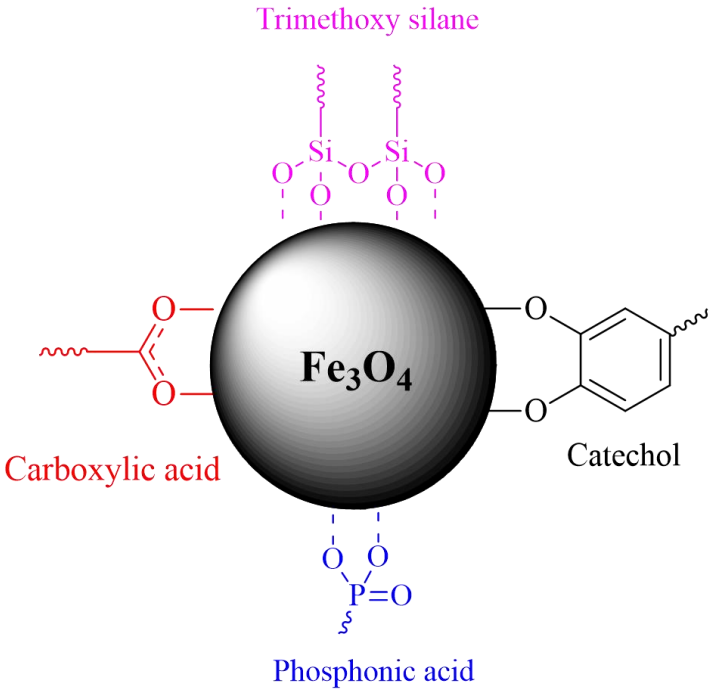

Figure 1.4. Anchoring groups for iron oxide nanoparticles.

Among these anchoring groups, catechol is the most widely used one. Because an experimental study from Rajh et al. has shown that dopamine (catechol) as a bidentate enediol ligand transfers the iron surface to lattice structure. And it also makes the geometry as octahedral which enables iron to coordinate with oxygen. [35] This situation finally results in a strong attachment between dopamine and iron oxide nanoparticles. According to Langmuir isotherms, it has been demonstrated that attachment of dopamine to iron oxide surface is preferable than detachment of it. [36] In addition, catechol is a bioinspired anchoring groups and it is very stable at high temperatures. Since it has an amine group in its structure, it can be attached to carboxylic acid bearing polymerization initiators easily. [37] Therefore, these features of dopamine make it very useful as an anchoring group.

1.4. Hydrophilic Coating of Iron Oxide Nanoparticles

Hydrophobic coatings of iron oxide nanoparticles need to be changed in order for them to be used for biological applications. In addition, iron oxide nanoparticles are more stable in aqueous media for a long time. Thus, polymerization of water soluble polymers is the first step for them to be made water dispersible. [38] There are some types of polymers that are attached to iron oxides for this reason. These polymers can be natural and they can be synthetic as well. For example, natural polymers are dextran, [39] starch, [40] gelatin [41] or chitosan. [42] Synthetic polymers are poly(ethylene glycol) (PEG), [43] poly(vinyl alcohol) (PVA), [44] poly(lactic acid) (PLA), [45] polymethylmethacrylate (PMMA) [46] or polyacrylic acid (PAA). [47]

Among the polymers shown above, the use of PEG has dramatically increased in recent years since PEG decreases attachment of undesired protein in biological environments. When it reduces this attachment to iron oxide nanoparticles, the circulation time of them can be increased. [48] In addition, it is a very flexible and hydrophilic molecule with a low toxicity. PEG polymers show biocompatible behaviors. Biocompatibility basically means a good guest-host response in a body. [49] In this context, PEG polymers show no adverse effects. In addition, the term “stealth nanoparticles” has given to PEGylated iron oxide nanoparticles because they cannot be detected by macrophages. And this situation makes it prolong for a long time in biological media. [50]

1.5. Polymer Grafting for Iron Oxide Nanoparticles

There are two types of approaches for polymers to be grafted in iron oxide nanoparticles. The first approach to do it is “grafting-to” approach and the other approach is “grafting-from” approach.

In grafting-to approach, polymers are grown and they are attached to the iron oxide nanoparticles covalently. In grafting–to approach, polymers need to have a reactive end

groups so that they can be attached to the nanoparticle surface. The density of the surface is not high since the polymers are able to fold and form a compact structure and this creates a steric hindrance. Steric hindrance limits the attachment of polymers. Since the polymers are grown before attaching to surface, they can be fully characterized. [51] This is an advantage of use of this approach. Figure 1.5. shows how the grafting-to approach works. First of all, polymers with reactive anchoring groups are synthesized. Then, oleic acid coated iron oxide nanoparticles and the polymers are mixed for conjugation. Oleic acids are replaced by polymers but since the polymers are bulk materials, not all the surface of iron oxides are coated by polymers.

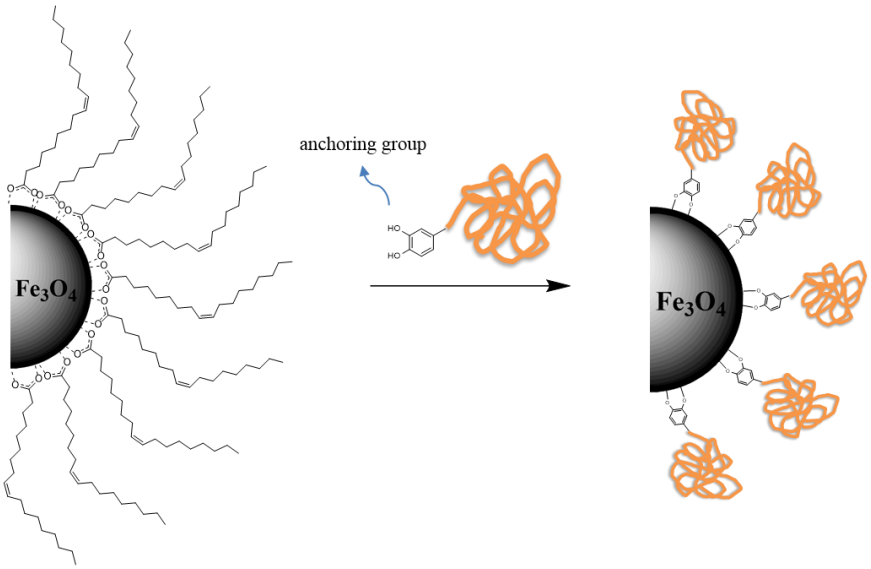

Figure 1.5. Grafting-to approach for iron oxide nanoparticles.

In contrast grafting-to approach, high density surface iron oxide nanoparticles can be synthesized by grafting-from approach. Polymers can be grown from the surface of iron oxide nanoparticles. Because a polymerization initiator is firstly immobilized to the surface. Then, polymerization starts with the initiator. This leads a high density surface. Although it seems to be very useful technique, the characterization of the polymers is difficult. [52] This is actually a disadvantage of this approach. Figure 1.6. shows grafting-from polymerization from the surface of iron oxide nanoparticles. First, oleic acid acids are replaced by initiators.

Then, polymerization occurs using these initiators. Finally, polymers are grown from the surface to yield a high density brush like coating on the surface.

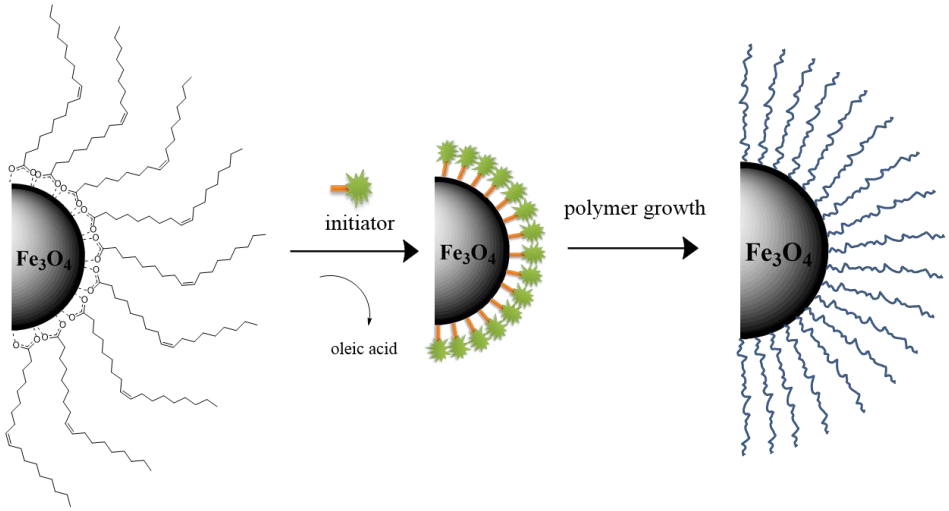

Figure 1.6 Grafting-from approach for iron oxide nanoparticles.

1.6. Reversible Addition-Fragmentation Chain-Transfer (RAFT) Polymerization

Polymers that are desired to be grafting to/from the surfaces can be synthesized by RAFT polymerization. This polymerization technique is widely used since it has some advantages. For example, it is suitable for most of the monomers. The polymerization can take place under mild conditions without use of any metal catalyst. After the polymerization, the end groups of the polymers can be modified by using radical exchange reactions. [53]

For RAFT polymerization to take place, a suitable chain transfer agent with a thiocarbonylthio group to control the molecular weight and PDI. [54] By using RAFT agent, a living polymerization can be obtained. A number of steps exist for this kind of polymerization. These steps start with initiation process and this step is followed by pre-equilibrium, re-initiation, main equilibrium, propagation. Finally, polymerization ends with termination process.

In the initiation process, the initiator is decomposed with heat to give radicals. The radical is usually AIBN. The radical reacts with the monomer to continue with the propagation. In the propagation step, the radical formed after initiation step react with number of monomers to grow the polymer chain. After propagation step, RAFT pre-equilibrium step follows. In this step, the growing chain reacts with the RAFT agent to give RAFT adduct radical. This is an equilibrium reaction where the RAFT adduct is able to lose it polymeric unit or the reactive group. The other step is initiation where the lost reactive group is able to form a radical by reacting with monomer. After this step, main RAFT equilibrium steps comes to grow the polymer chain by sharing the radicals before reaching the termination step. Finally, the polymers with their radical ends react with each other to terminate the polymerization. This step is called termination step. [55] The steps of RAFT polymerization are given in Figure 1.7.

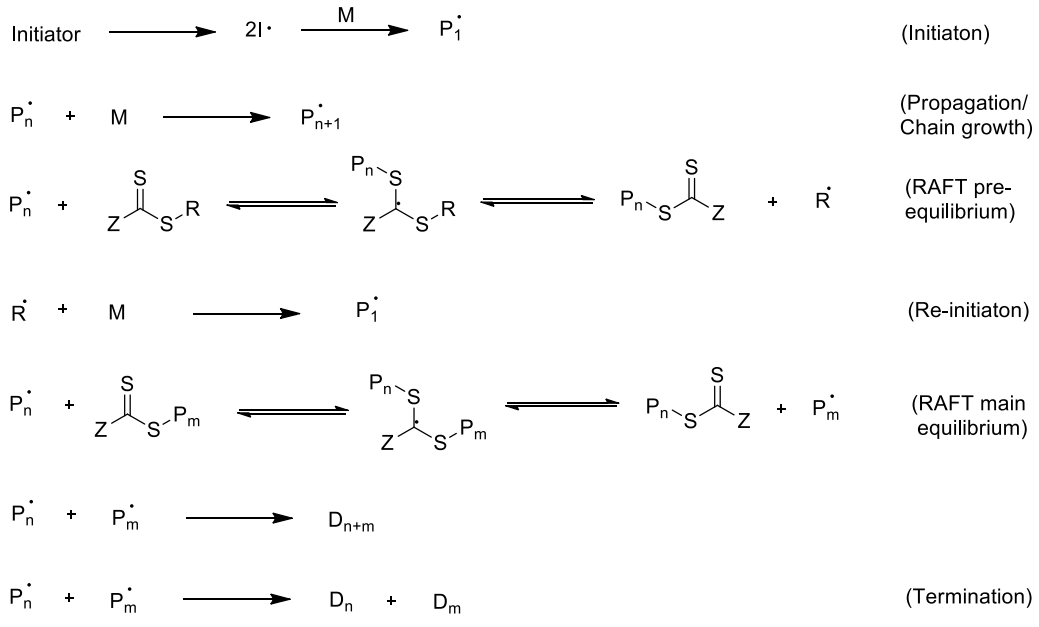

Figure 1.7. Steps of RAFT polymerization. [56]

1.7. End Group Modification after RAFT Polymerization

After the synthesis of polymers by RAFT polymerizations, the end groups of these polymers are R or Z depending on what type of chain transfer agent is used. These R and Z end groups can be replaced by end group modifications. [57] Polymers with functional groups can be synthesized by benefiting from this feature of RAFT agents. The existence of thiocarbonylthio group that is used for RAFT polymerization is able to be modified after polymerization. One of the techniques to change the end group of these polymers is radical cross coupling reaction.

In order for polymer end groups to be modified, an azo initiator is needed as a radical source. For this reason, a functionalized azo initiators are synthesized to make the polymers be used for many biological applications. [58] For example, it has been published that trithiocarbonate groups of iron oxide nanoparticles were modified by protected maleimide and azide functionalized azo initiator. After radical cross coupling reaction with functional azo initiator, protected maleimide was made deprotected by heating. Then thiol and alkyne containing dyes attached accordingly. The synthesis is shown in Figure 1.8.

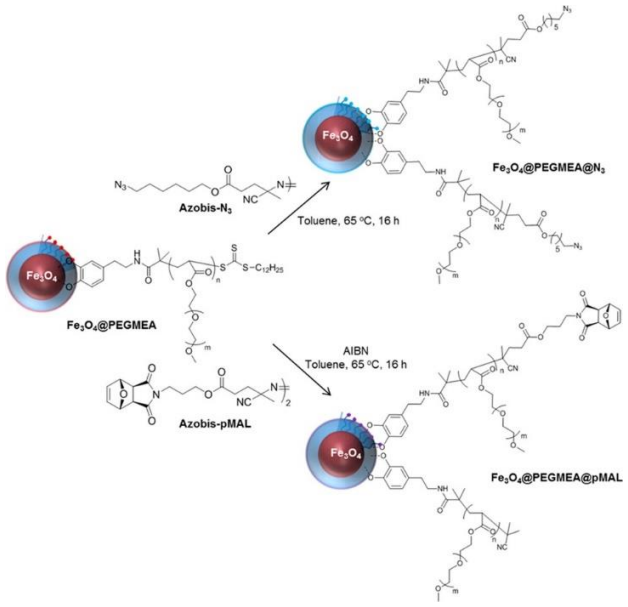

Figure 1.8. Functionalization of polymer-coated iron oxide nanoparticles with protected maleimide and azide groups by radical exchange reaction. [59]

These azo initiators can be diversified according to the applications. For example, the azo initiators can be functionalized with azide, activated carboxylic acid or pyridyl disulfide groups by formation of esters or amides.

1.8. Functionalization of End Groups with Disulfide Bond and Activated Carboxylic Acid

1.8.1. Activated Carboxylic Acid and Amine Reaction

N-Hydroxysuccinimide is a reagent used to activate carboxylic acids to react them with amines to form amides. [60] By using this chemistry, amine containing materials can be easily conjugated to activated acids without using any other reagents. For example, amine containing targeting group can be attached to activated carboxylic acid containing polymer to form a robust amide bond shown in Figure 1.9. Amide bonds are resistant to degradation. That means breakage of amide bonds is not as easy as that of esters. [61] It is important to have an irreversible conjugation. [62] Because the conjugation bond should not be hydrolyzed until the targeting group accumulates in the desired place in the body.

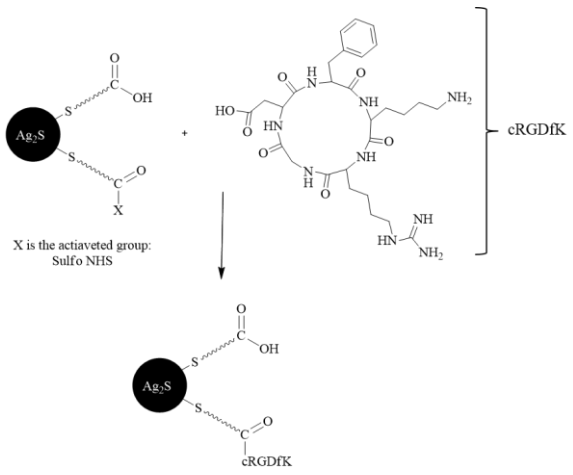

Figure 1.9. Conjugation of cRGDfK to NHS activated carboxylic acid containing QDs by amide formation. [63]

1.8.2. Thiol-Disulfide Exchange Reaction

In recent years, the use of disulfide groups in biological applications has increased dramatically due to the fact that they react with thiol containing compounds such as a protein, drug or targeting group to form a disulfide bond after conjugation. [64] Whether the conjugation of a material to polymers is reversible or irreversible is important for release of that material. The main advantage of using disulfide bonds in biological applications is that the conjugation is reversible. A drug/peptide attached or loaded to polymers can be released in the presence of a free thiol shown with an example in Figure 1.10. This situation makes the attached material active in biological environments.

It is important to attach a biological material that is intended to be released from a polymer with disulfide bond. Because the amount of glutathione found in cancer cells is higher than that of normal cells. [65] Glutathione is a natural compound having free thiol in its structure. It gives resistance to cancer cells to protect themselves from cancer drugs. [66] By using this chemistry, cancer cells can be killed by therapeutic compounds.

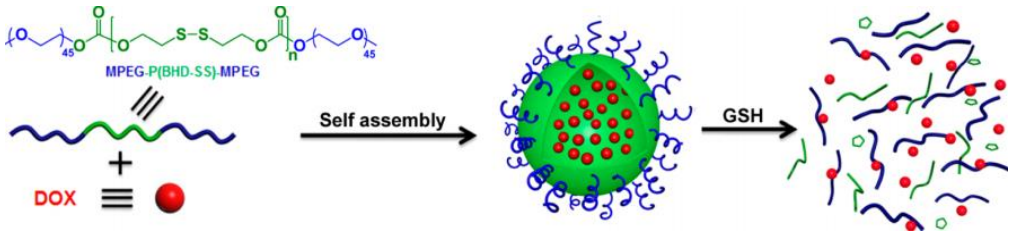

Figure 1.10. Disulfide exchange reaction between disulfide containing polymer and glutathione. [67]

2. FABRICATION OF MAGNETIC NANOPARTICLES WITH CLEAVABLE POLYMER BRUSHES

2.1. Aim of the Study

The aim of this project is to synthesize two types of water dispersible polymer-coated iron oxide nanoparticles with functional end groups. One type of polymer grafted iron oxide nanoparticle has cleavable disulfide group that bridges between iron oxide and grafted polymers. The other type lacks of this disulfide group. It is difficult to determine the features of the polymers grown by grafting-from method. Therefore, we aimed to characterize the polymers which can be cleaved from the iron oxide nanoparticles to know their molecular weights and polydispersity indexes in mild condition. BODIPY dye conjugated monomer as a drug model and PEG are copolymerized after characterization of grafted polymers. The reason why a dye molecule in polymer chain is used is to show that a hydrophobic molecule can be conjugated to a hydrophilic molecule and making the dye hydrophilic as well. The end groups of these polymers are replaced by activated esters for the future amine conjugation.

For the synthesis of such novel molecules, monodisperse iron oxide nanoparticles were synthesized at high temperatures. Catechol based chain transfer agents with and without disulfide bonds were synthesized and immobilized onto iron oxide nanoparticles. After immobilization, PEG based hydrophilic polymers were synthesized by grafting from approach. Disulfide containing polymer-coated iron oxide nanoparticles were cleaved to be separated in the presence of a reducing agent. Time dependent molecular weights and PDI values were determined.

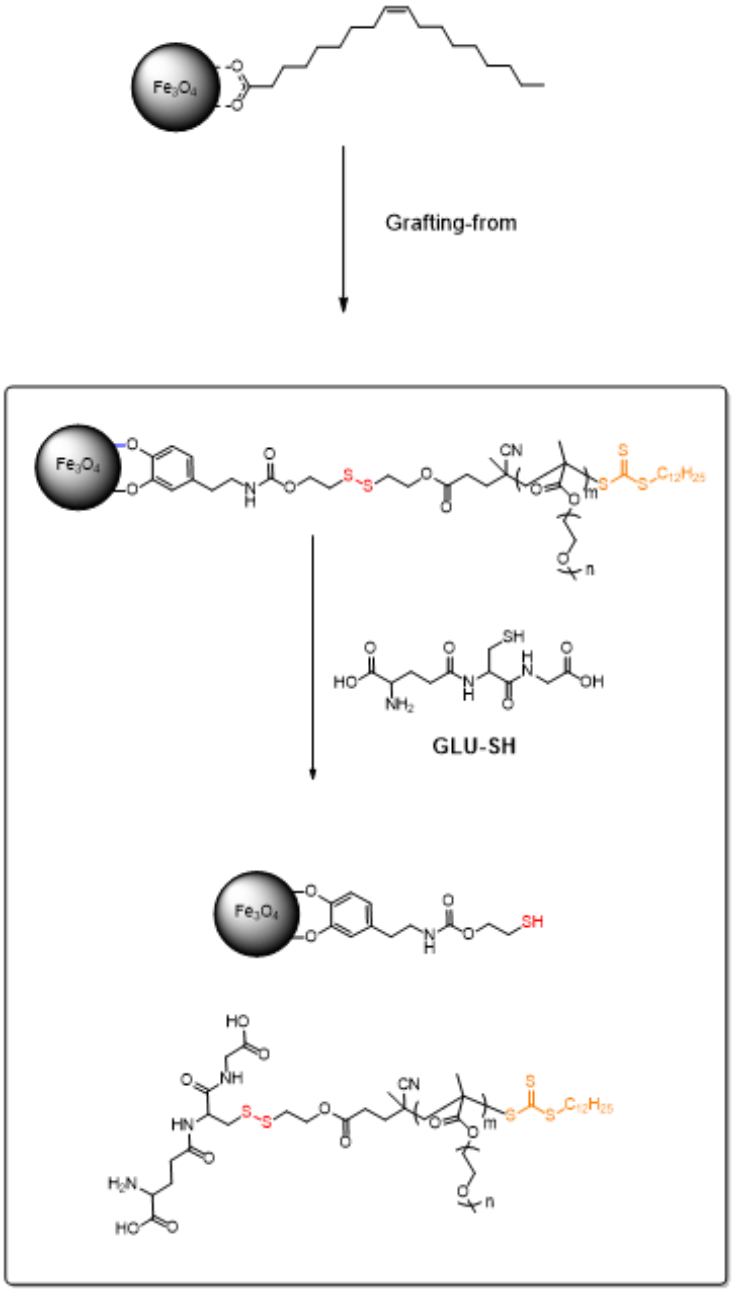

Figure 2.1. General scheme of the project.

3. EXPERIMENTAL

3.1. Materials

Oleic acid, dopamine hydrochloride, 1-dodecanethiol, iron (III) chloride hexahydrate, DMAP, DSC (>95%), 1-amino-2-propanol, L-Glutathione reduced and fluorescein amine, isomer I were purchased from Sigma-Aldrich. No purification was needed for these compounds. Sodium oleate was purchased from TCI. Triethylamine, 2,2'-disulfanediyldiethanol, EDCI, AIBN (recrystallization in ethanol before use), DTT, cysteamine, 1-octadecene, DCC and NHS were purchased from Alfa-Aesar. Poly (ethylene glycol) methyl ether methacrylate (PEGMEMA) was purchased from Sigma-Aldrich and basic aluminum oxide was used for purification. V-501 and CS_2 were purchased from Fluka. Toluene, THF, EtOAc, methanol, DMF, DCM, chloroform, hexane and ethanol were purchased from Merck. BODIPY-SH was synthesized according to the literature example. [68] cRGDfK was synthesized using solid phase peptide synthesis (SSPS, PS3 Peptide Synthesizer, Protein Technologies Inc., USA). The KLAK peptide was purchased from Royobiotech Limited with 95.2% purity.

3.2. Instrumentation

^{1}H NMR spectra were obtained using 400 MHz Bruker spectrometer at 25^{o}C. Deuterated chloroform was used as the NMR solvent. Fourier transform infrared (FT-IR) spectra were obtained by using Thermo Scientific Nicolet 380. Gel permeation chromatography with a PSS-SDV column (Gram linear, length/ID 8x300 mm, 10 µm particle size) was used to determine the molecular weights and PDI values of the grafted polymers. Dimethylacetamide was used as the eluent. UV-visible spectra were obtained using Varian Cary 100 Scan spectrophotometer. Malvern Zetasizer Nano ZS photometer was used to obtain dynamic light scattering (DLS) results. Hexane and DMF were used as the

solvents at 20 ^{o}C. Iron oxide nanoparticle images were obtained using transmission electron microscopic (TEM) having LVEM5 microscope.

3.3. Iron Oxide Nanoparticles Synthesis

Iron oxide nanoparticles are synthesized in two steps and the procedure of this reaction was taken from the literature. [22] First of all, iron oleate complex was synthesized and this compound reacted with oleic acid in the presence of a high boiling solvent to get oleic acid stabilized monodisperse iron oxide nanoparticles.

3.4. Synthesis of Dopamine Modified Chain Transfer Agent (CTA)

3.4.1. Synthesis of 4-cyano-4-(((dodecylthio)carbonothioyl)thio) pentanoic acid (CTA)

The chain transfer agent (CTA) that was intended to be modified with dopamine was synthesized according to the literature.[69]

3.4.2. Synthesis of 2,5-dioxopyrrolidin-1-yl 4-cyano-4-((dodecylthio) carbonothioyl)-thio) pentanoate (CTA-NHS)

CTA-Succinimide ester (CTA-NHS) and CTA-Dopa was synthesized according to the literature example. [70]

3.4.3. Synthesis of 2- cyano-5- ((3,4-dihydroxyphenethyl)amino)-5-oxopentan-2-yl dodecyl carbonotrithioate (CTA-Dopa)

In order to synthesize dopamine modified CTA, Dopamine.HCl (375 mg, 1.98 mmol) and TEA (218 mg, 2.16 mmol) were dissolved in 5 mL of DMF. This mixture was stirred

for 15 minutes at room temperature. Then, CTA-NHS (800 mg, 1.6 mmol) was added and this obtained reaction mixture was stirred at room temperature for 48 hours under dark environment. At the end of the reaction, the mixture was dropped into phosphate buffer (100 mL, pH 4.0). The precipitated yellow solid was collected by filtration method. And it was lyophilized to remove water. Then, this solid was purified by column chromatography using ethyl acetate/ hexane (2:3) (328 mg, 38% yield). ^{1}H NMR ($CDCl_3$) δ (ppm): 6.82 (d, 1H), 6.70 (s, 1H), 6.60 (d, 1H), 5.65 (s, 1H), 3.48 (t, 2H), 3.32 (t, 2H), 2.70 (t, 2H), 2.48 (m, 1H), 2.44 (t, 2H), 2.31 (m, 1H), 1.84 (s, 3H), 1.68 (m, 2H), 1.34 (m, 18H), 0.88 (t, 3H).

3.5. Synthesis of Disulfide Containing Chain Transfer Agent

3.5.1. Synthesis of (S)-2-((2-hydroxyethyl)disulfanyl) ethyl 4-cyano-4-(((dodecylthio) carbonothioyl)thio)pentanoate (CTA-SS-OH)

CTA-SS-OH compound is synthesized according to the literature example.[71] It was obtained by the esterification reaction between CTA (shown in Chapter 1) and 2,2'-disulfanediyldiethanol. CTA ((S)-4-cyano-4-(((dodecylthio)carbonothioyl)thio)pentanoic acid) (1 g, 2.48 mmol) was dissolved in 5 mL of dry CH_2Cl_2 on top of an ice bath. DCC (614 mg, 2.98 mmol) was dissolved in 3 mL of CH_2Cl_2. Then, this mixture was combined with CTA solution. The resulting mixture was stirred for 10 minutes. After that, 2,2'-disulfanediyldiethanol (382 mg, 2.48 mmol) was added to the mixture drop by drop. Finally, DMAP (30 mg, 0.248 mmol) which was dissolved in 1 mL of EtOAc was added to final mixture. The temperature of this mixture was allowed to come to room temperature. Then, it was stirred at room temperature for 24 hours. After the reaction, the white solid (DCU) which is a by-product of this reaction was removed by filtration. Then, in order to purify the compound, the mixture was extracted with 25 mL of 0.1 M HCl and brine twice. Then, the organic part was dried over Na_2SO_4. The solvent was vacuumed by rotary evaporation. Obtained yellow viscous liquid was purified by column chromatography using ethyl acetate (15 %) / hexane (85 %) (696 mg, 52% yield). ^{1}H NMR ($CDCl_3$) δ (ppm): 4.38 (t, 2H), 3.90 (t, 2H), 3.33 (t, 2H), 2.94 (t, 2H), 2.89 (t, 2H), 2.64 (t, 2H), 2.53 (m, 1H), 2.39 (m, 1H), 1.88 (s, 3H), 1.68 (m, 2H), 1.21-1.41 (m, 18H), 0.88 (t, 3H).

3.5.2. Synthesis of (S)-2-((2-((((2,5-dioxopyrrolidin-1-yl)oxy)carbonyl) oxy) ethyl) disulfanyl) ethyl 4-cyano-4-(((dodecylthio)carbonothioyl)thio)pentanoate (CTA-SS-DSC)

CTA-SS-DSC compound was synthesized using CTA-SS-OH and DSC molecule to get activated carboxylic acid for the next amine conjugation. For this synthesis, CTA-SS-OH (400 mg, 0.741 mmol) and DSC (342 mg, 1.33 mmol) and TEA (75 mg, 0.741 mmol) were mixed in 10 mL of dry CH_2Cl_2. The reaction mixture was stirred at room temperature for 24 hours. In order to purify this compound, the mixture was extracted with 20 mL of saturated $NaHCO_3$ and brine twice. Organic part was dried over Na_2SO_4. The solvent was removed using rotary evaporation.

3.5.3. Synthesis of (S)-2- ((2- (((3,4- dihydroxyphenethyl)carbamoyl)oxy)ethyl) disulfanyl)ethyl 4-cyano-4-(((dodecylthio)carbonothioyl)thio)pentanoate (CTA-SS-Dopa)

CTA-SS-Dopa compound was synthesized using CTA-SS-DSC and dopamine hydrochloride. For the synthesis, CTA-SS-DSC (250 mg, 0.367 mmol) was dissolved in 5 mL of dry DMF. Then, dopamine hydrochloride (73 mg, 0.385 mmol) was dissolved in 1.5 mL of dry DMF and it was added to previous solution dropwise. After this step, TEA (74 mg, 0.734 mmol) was added to final mixture drop by drop. The mixture was stirred at room temperature for 48 hours. In order to purify the desired compound, reaction mixture was extracted with 10 mL of 1 N HCl and $NaHCO_3$ twice. Organic part was dried over Na_2SO_4. The solvent was removed by rotary evaporation.

3.7. Synthesis of (E)-bis(2,5-dioxopyrrolidin-1-yl) 4,4'-(diazene-1,2-diyl)bis(4-cyanopentanoate) (NHS-ACVA)

This compound was synthesized according to the literature.[72] For this synthesis, V501 (500 mg, 1.78 mmol), NHS (548 mg, 4.76 mmol) were dissolved in 5 mL of dry DMF. To this solution, EDCI (913 mg, 4.76 mmol) which was dissolved in 4 mL of dry DMF was

added at 0 ^{o}C for 1 hour. Then, the reaction mixture was allowed to stir at room temperature for 36 hours. In order to purify this NHS-ACVA, the reaction mixture was dropped into 400 mL of distilled water. White solid precipitation was observed and this precipitate was collected by filtration method. The product was lyophilized for 24 hours to remove water. Finally, white solid product was obtained (760 mg, 90% yield). ^{1}H NMR ($CDCl_3$) δ (ppm): 2.84 (s, 8H), 2.95-2.75 (m, 4H), 2.71-2.49 (m, 4H), 1.78 - 1.71 (s, 6H).

3.8. Place Exchange Reaction between Fe_3O_4@OA and Dopa-CTA (Fe_3O_4@Dopa-CTA)

The ligand exchange reaction procedure was done according to the literature.[59] For this synthesis, oleic acid stabilized Fe_3O_4 nanoparticles (Fe_3O_4@OA) (30 mg) was dissolved in 3 mL of chloroform. Then, Dopa-CTA (150 mg, 0.278 mmol) was added to this solution. The final mixture was allowed to stir at 40 ^{o}C for 48 h under nitrogen environment. After the reaction, the solvent was partially removed by rotary evaporation. Then, as the purification of part, 30 mL of methanol was added to this mixture to precipitate the desired product (Fe_3O_4@Dopa-CTA) until all free Dopa-CTA was removed. After that, the product was kept in 1 mL of $CHCl_3$ for the future reactions.

3.9. Place Exchange Reaction between Fe_3O_4@OAand CTA-SS-Dopa (Fe_3O_4@Dopa-SS-CTA)

CTA-SS-Dopa molecule was immobilized into the iron oxide nanoparticles by ligand exchange reaction. For this reaction, CTA-SS-Dopa (150 mg) was mixed with oleic acid stabilized iron oxide nanoparticles (30 mg) in chloroform (3 mL). The resulting mixture was stirred at 40 °C for 48 hours under nitrogen blanket. After the reaction, the solvent was evaporated to a volume of until 1 mL. Then, this was precipitated in methanol (30 mL). The methanol-chloroform mixture was centrifuged (7000 rpm, 10 minutes) and wash was repeated until all unreacted CTA-SS-Dopa was removed. Finally, thus obtained black product was stored in $CHCl_3$ until further use.

3.10. RAFT Polymerization of PEGMEMA from the Surface of Fe_3O_4 Nanoparticles (Fe_3O_4@Dopa-PEGMEMA)

The procedure for surface-initiated RAFT polymerization of PEGMEMA was taken from the same literature where the previous synthesis was done.[59] For this polymerization, Fe_3O_4@Dopa-CTA (10 mg), PEGMEMA (500 mg, 1.67 mmol) and AIBN (1.1 mg, 6.68 x 10^{-3} mmol) were dissolved in toluene (3 mL). Then, the reaction mixture was purged with N_2 for 20 minutes to remove O_2 from the reaction environment. After that, reaction mixture was allowed to stir at 70 °C for 24 hours. After polymerization, the solvent was removed by rotary evaporation. Then, the polymers were precipitated in cold diethyl ether (3 times) to remove unreacted monomers. Finally, a black viscous product was obtained.

3.11. RAFT Polymerization of PEGMEMA from the Surface of Fe_3O_4 Nanoparticles (Fe_3O_4@Dopa-SS-PEGMEMA)

RAFT polymerization was done on the surface of iron oxide nanoparticles by using PEGMEMA as the monomer. For this reason, 10 mg of Fe_3O_4@Dopa-SS-CTA was mixed with PEGMEMA (500 mg, 1.67 mmol) and AIBN (1.1 mg, 6.68x10^{-3} mmol). The obtained mixture was dissolved in 3 mL of toluene. This mixture was purged with N_2 for 20 minutes to remove O_2 gas from the reaction mixture. Finally, the reaction was stirred at 75 °C for 8, 16 and 24 hours in order to measure the molecular weights of the polymers grown from the surface depending on time. This polymerization process was repeated 3 times for 8, 16 and 24 hours. After the reaction, solvent was removed by rotary evaporation. The obtained black viscous product was precipitated in cold diethyl ether to remove unreacted monomers.

3.12. Reductive Cleavage of PEGMEMA Polymers from Fe_3O_4 Nanoparticles and

DTT was used in order to cleave the disulfide bond that builds a bridge between and nanoparticles and polymers. For this cleavage reaction, 20 mg of Fe_3O_4@Dopa-SS-PEGMEMA and DTT (1.54 mg, 0.01 mmol) were dissolved in phosphate buffer (1 mL) solution (pH= 8.0). Resulting mixture was stirred at room temperature for 1 hour. In order

to separate iron oxide nanoparticles and polymers, reaction mixture was added into water (9 mL) and the solution was centrifuged at 9000 rpm for 15 minutes. Iron oxide nanoparticles precipitated since they were no longer dispersible in water. However, hydrophilic polymers dissolved in water and could be obtained through lyophilization.

4. RESULTS AND DISCUSSIONS

4.1. Synthesis of Fe_3O_4 Nanoparticles

Thermal decomposition method was used to synthesize magnetic Fe_3O_4 nanoparticles to be able to control the size and polydispersity. The synthesis of these nanoparticles has two steps. The first step is the synthesis of iron oleate complex by using iron (III) chloride and sodium oleate salt as precursors (Figure 4.1).

$$FeCl_3.6H_2O + 3\ \text{Sodium Oleate} \xrightarrow[70\ ^{o}C,\ 4\ h]{\text{Ethanol, Water, Hexane}} Fe(oleate)_3 + 3\ NaCl + 6H_2O$$

Figure 4.1. The synthesis of iron oleate complex.

The second step is done by using iron oleate complex and oleic acid in the presence of a high boiling solvent 1-octadecene (Figure 4.2). Iron oxide nanoparticles are stabilized by oleic acid to prevent them from agglomeration.

$$Fe(oleate)_3 + \text{Oleic Acid} \xrightarrow[320\ ^{o}C,\ 30\ \text{mins}]{\text{1-octadecene}} Fe_3O_4@OA$$

Figure 4.2. Synthesis of iron oxide nanoparticles.

The characterization of these oleic acid-coated magnetic nanoparticles was achieved by using FT-IR spectroscopy, transmission electron microscopy (TEM) and dynamic light scattering (DLS) (Figure 4.3). The peaks at 2920 and 2851 cm^{-1} correspond to the symmetric and asymmetric $–CH_2-$, respectively. The peak at 550 cm^{-1} comes from the Fe-O bonds of

iron oxide molecules. Their average sizes determined using DLS were around 10 nm (diameter). Similarly, TEM results also showed similar sizes around 11 nm.

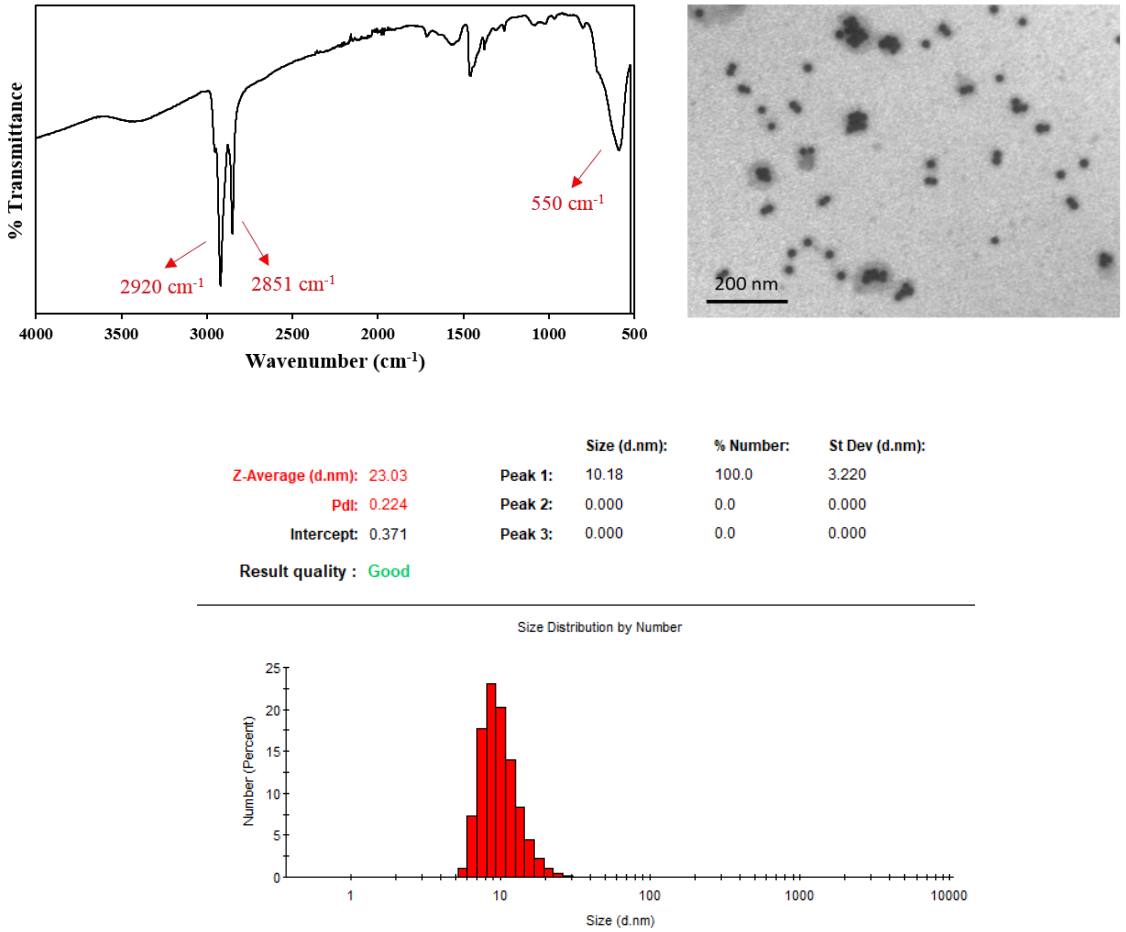

Figure 4.3. FT-IR spectrum (left) and TEM image (right) and DLS analysis (bottom) of Fe_3O_4@OA.

4.2. Synthesis of Chain Transfer Agent (CTA)

A chain transfer agent (CTA) is needed in order to grow polymers from the surface of magnetic iron oxide nanoparticles. For this purpose, trithiocarbonate containing CTA was synthesized to be used for RAFT polymerization according to literature procedure (Figure 4.4).[69] Since the chain transfer agent has trithiocarbonate group in its structure, this group can be modified to functional groups by radical exchange reactions.

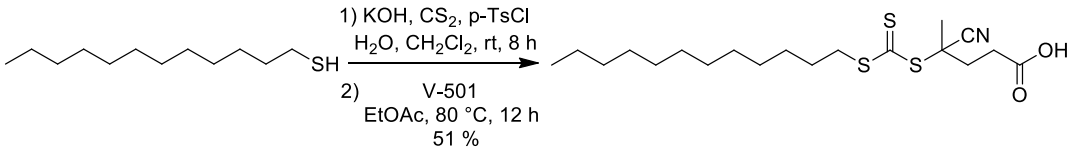

Figure 4.4. Synthesis of chain transfer agent (CTA).

4.3. Synthesis of Dopamine Modified Chain Transfer Agent (Dopa-CTA)

In order to attach the chain transfer agent to iron oxide nanoparticles, an anchoring group is required. For that purpose, dopamine was chosen as the anchoring group. First of all, the chain transfer agent is activated by NHS in the presence of EDCI and CH_2Cl_2 as the solvent to get NHS-CTA. This NHS-CTA was used for the conjugation of dopamine. For this reaction, NHS-CTA and dopamine hydrochloride were used in the presence of TEA and DMF as the solvent (Figure 4.5). The yield of this reaction was calculated as 38 %. The characterization of this compound was done with ^{1}H NMR (Figure 4.6) and was determined to be similar to previously reported. [70] The peaks at 6.82, 6.70, 6.60 ppm come from the benzene ring of dopamine. In addition, the peak at 5.65 ppm comes from the amide bond between dopamine and CTA, which shows the successful conjugation of dopamine.

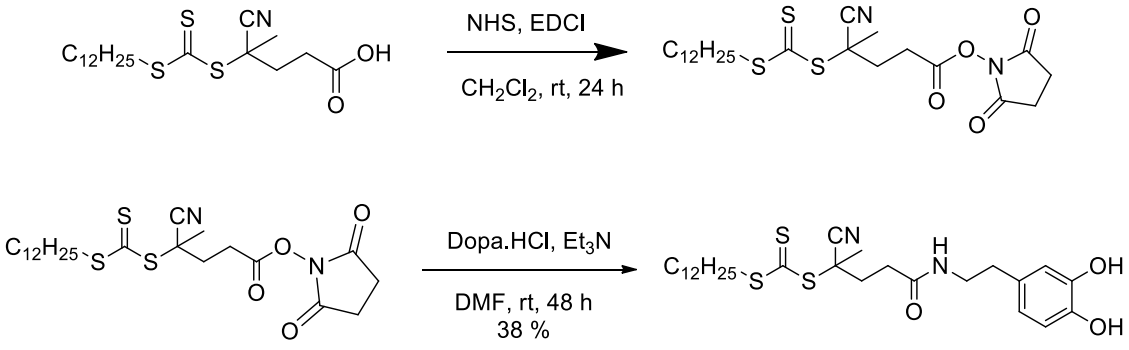

Figure 4.5. Synthetic route of dopamine modified chain transfer agent (Dopa-CTA).

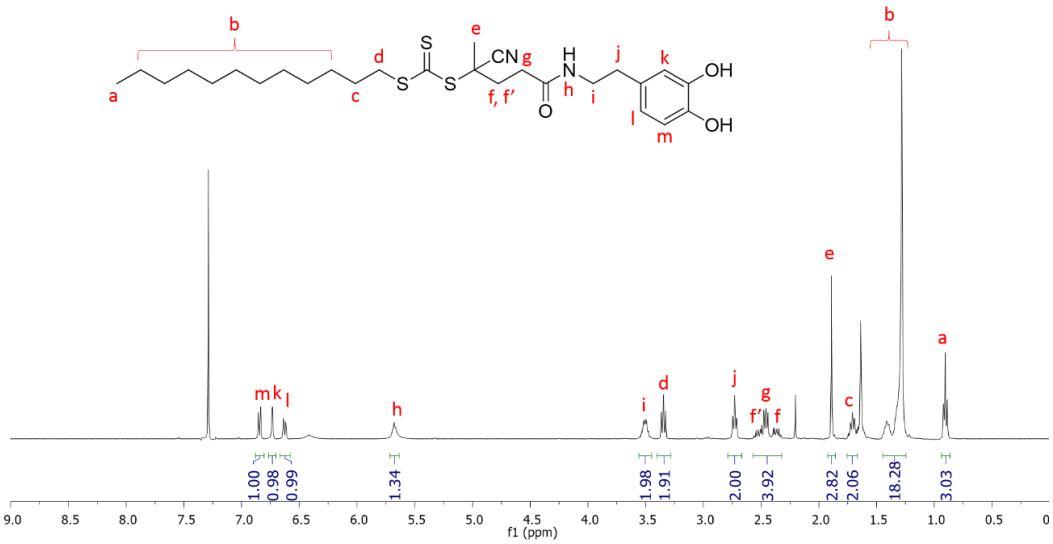

Figure 4.6. ^{1}H NMR spectrum of Dopa-CTA.

4.4. Synthesis of CTA-SS-OH

In order to immobilize the chain transfer agent to the iron oxide nanoparticles, dopamine needs to be conjugated to CTA. This synthesis consists of a couple of reactions. The first one is to convert carboxylic acid containing CTA into alcohol. For this reason, 2,2'-disulfanediyldiethanol which is a diol was used to make CTA become an alcohol (Figure 4.7). The reaction is an esterification reaction in the presence of DCC, DMAP and CH_2Cl_2 as the solvent. The yield of this reaction was calculated as 52 %. Characterization of this compound was done with ^{1}H NMR (Figure 4.8). The presence of the characteristic peak at 4.38 ppm belonging to the protons adjacent to the carbon oxygen bond between the CTA and diol indicates successful conjugation.

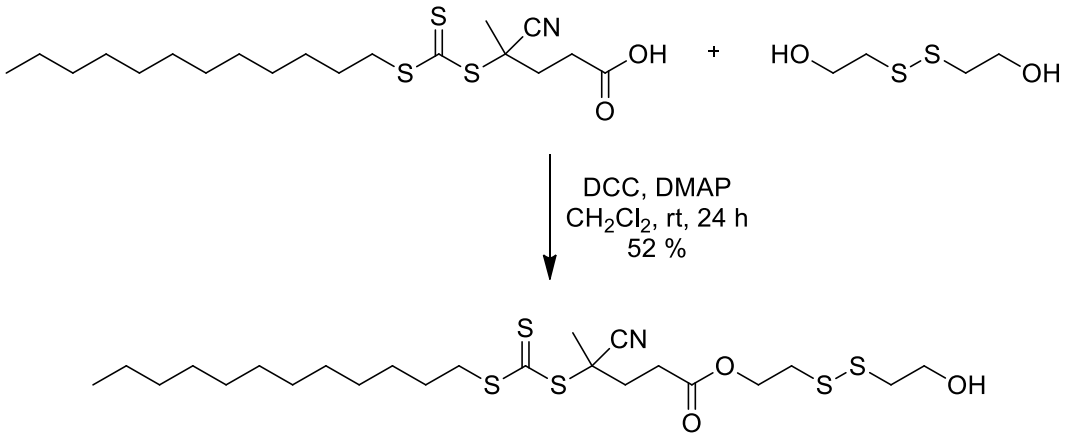

Figure 4.7. Synthesis of CTA-SS-OH.

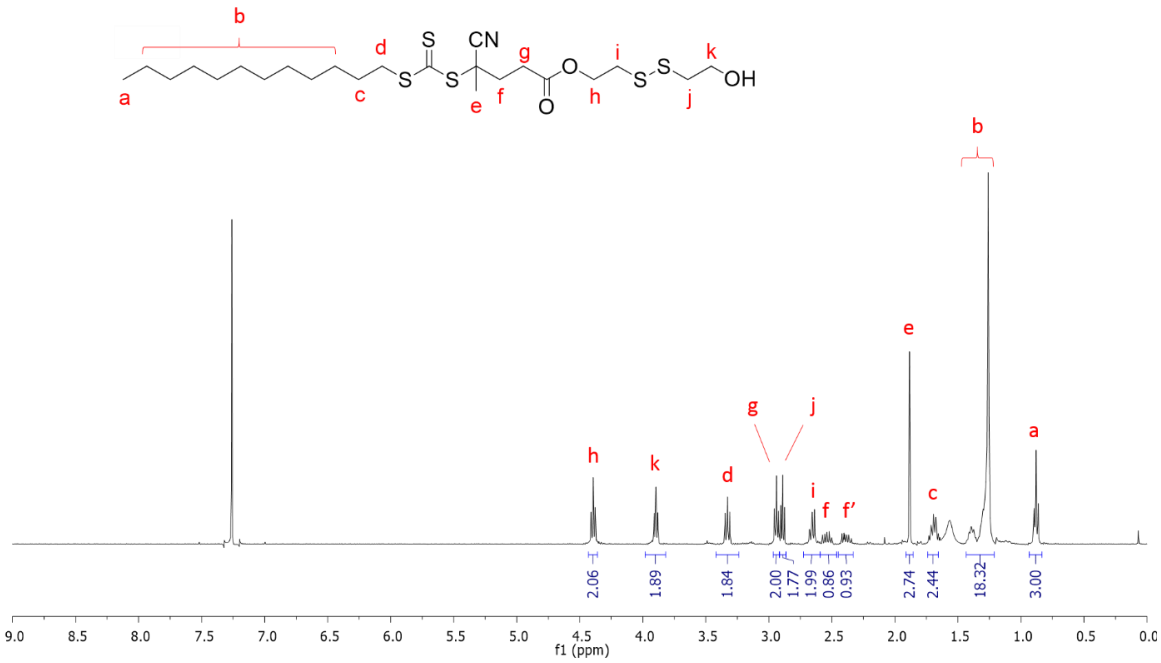

Figure 4.8. ^{1}H NMR spectrum of CTA-SS-OH.

4.7. Synthesis of NHS Containing Carboxylic Acid Functionalized V-501 Azo Initiator (NHS-ACVA)

The aim of synthesizing this molecule is to modify the trithiocarbonate groups of the surface initiated polymers as NHS-activated carboxylic acid groups using radical exchange reaction. The synthesis of this molecule was undertaken according to previous literature report.[72] The NHS-activated carboxylic acid containing azo-initiator is the product of esterification reaction V-501 azo-initiator and NHS in the presence of EDCI and DMF as the solvent (Figure 4.9). The reaction was carried out at room temperature to yield the desired product in high yield (95 %). NHS-ACVA molecule was precipitated in excess amount of water. The characterization of this compound was done with ^{1}H NMR (Figure 4.10). The peak at 2.85 ppm belongs to the protons of NHS ring, whereas the peaks at 1.77 and 1.73 ppm originate from the methyl groups of the V-501 azo-initiator. Presence of all desired peaks indicate successful conjugation of NHS functional group to the azo initiator.

Figure 4.9. Synthesis of NHS-ACVA radical initiator.

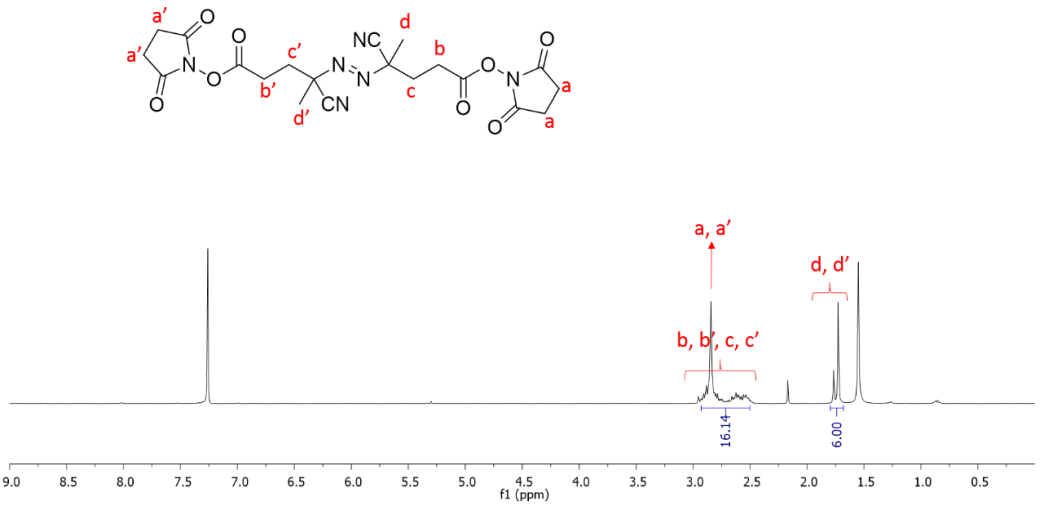

Figure 4.10. ^{1}H NMR spectrum of NHS-ACVA azo-initiator.

4.8. Immobilization of Chain Transfer Agent (Dopa-CTA) onto Fe_3O_4 Nanoparticles by Ligand Exchange Reaction (Fe_3O_4@Dopa-CTA)

To be able to grow polymers from the surface of magnetic Fe_3O_4 nanoparticles, immobilization of chain transfer agent is required. For this purpose, dopamine modified CTA (Dopa-CTA) was attached to iron oxide nanoparticle surface by ligand exchange reaction. This molecule is synthesized by using Fe_3O_4@OA and excess amount of Dopa-CTA in the presence of CH_2Cl_2 at 40 °C under N_2 (Figure 4.11). After the reaction, Fe_3O_4@Dopa-CTA was precipitated in methanol until all free Dopa-CTA is removed. Once the purification is done, the molecule was kept in chloroform to prevent them from aggregation.

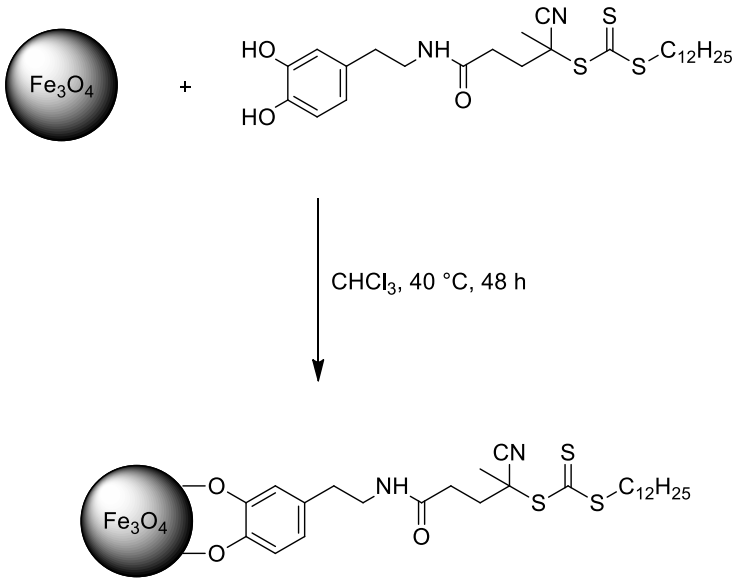

Figure 4.11. Synthesis of Fe_3O_4@Dopa-CTA.

The characterization of this molecule was carried out with FT-IR, UV spectroscopy and DLS. The peak at 1641 cm^{-1} comes from amide carbonyl group of Dopa-CTA and the peak at 550 cm^{-1} comes from Fe-O bond. FT-IR proves the immobilization of Dopa-CTA onto the nanoparticle surface. Then, UV spectroscopy was used to see the existence of Dopa-CTA. The immobilized molecule gives a shoulder-like peak at 320 nm and iron oxide gives a sharp peak at 250 nm. These also prove that Dopa-CTA molecule was successfully attached to iron oxide molecule (Figure 4.12). According to DLS results, Fe_3O_4@Dopa-CTA nanoparticles have a diameter of 13.7 nm.

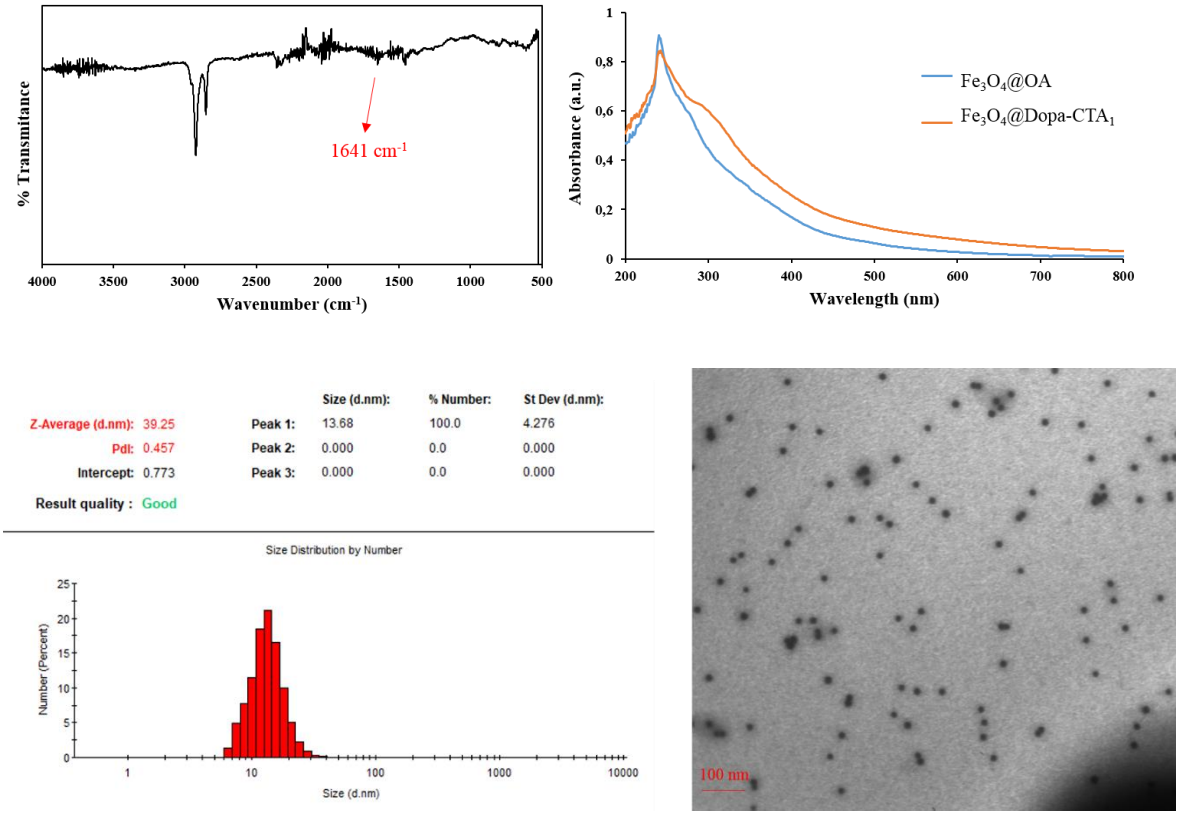

Figure 4.12. FT-IR spectrum (top left), UV spectroscopy (top right), DLS analysis (bottom left) and TEM image (bottom right) of Fe_3O_4@Dopa-CTA.

4.9. Immobilization of Chain Transfer Agent (Dopa-SS-CTA) onto Fe_3O_4 Nanoparticles by Ligand Exchange Reaction (Fe_3O_4@Dopa-SS-CTA)

CTA-SS-Dopa molecule was immobilized onto iron oxide nanoparticles by ligand exchange reaction (Figure 4.13). Disulfide containing dopamine modified CTA was attached to iron oxide nanoparticles for polymers to be grown from the surface. This molecule was synthesized using oleic acid stabilized iron oxide nanoparticles and excess amount of CTA-SS-Dopa molecule. After the reaction, reaction mixture was precipitated in methanol to remove excess amount of CTA-SS-Dopa. The obtained product was stored in $CHCl_3$ to eliminate the aggregation of nanoparticles.

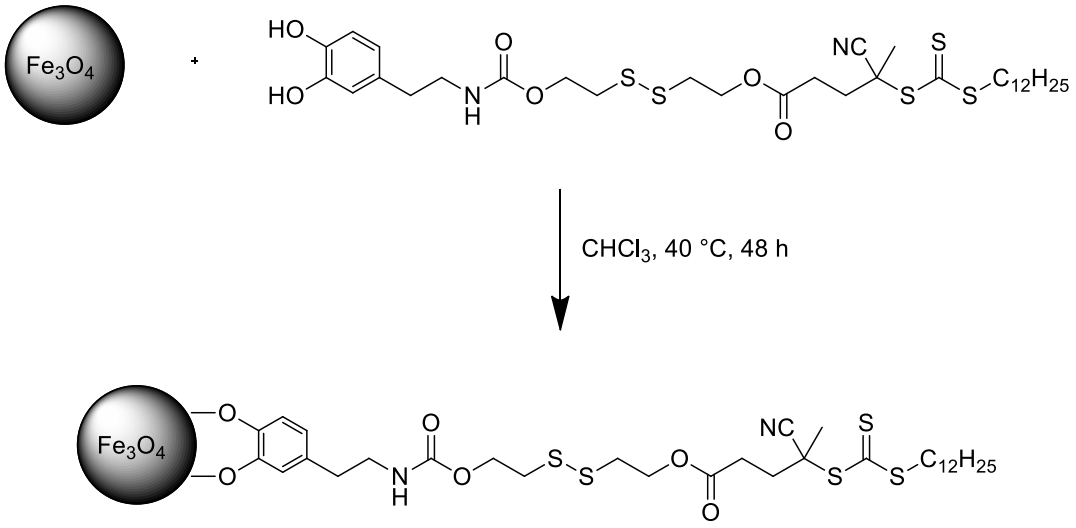

Figure 4.13. Ligand exchange reaction between Fe_3O_4@OA and CTA-SS-Dopa.

Characterization of this molecule was achieved using FT-IR, DLS, TEM and UV spectroscopy. The new shoulder like peak at 280 nm originates from the surface immobilized chain transfer agent. In FT-IR, the peak at 1641 cm^{-1} belongs to the amide carbonyl group. In addition, the peak at 550 cm^{-1} belongs to the Fe-O bond (Figure 4.14). This information shows that the conjugation of chain transfer agent to iron oxide nanoparticles is successful. According to DLS results, Fe_3O_4@Dopa-SS-CTA molecule has the diameter of 14.4 nm.

4.10. Surface Initiated RAFT Polymerization of PEGMEMA (Fe_3O_4@Dopa-PEGMEMA)

Once the chain transfer agent is immobilized onto iron oxide nanoparticles, RAFT polymerization of PEGMEMA was carried out. The reason the PEGMEMA was used as the monomer is that when it polymerizes it provides an anti-biofouling and biocompatible coating. Polymers were grown from the surface of nanoparticles by grafting-from approach. For this synthesis, Fe_3O_4@Dopa-CTA, PEGMEMA monomers and AIBN as the initiator were used and they were dissolved in toluene. The reaction mixture was purged with N_2 and stirred at 70 °C for 24 hours (Figure 4.15). Once the reaction was complete, the reaction mixture was precipitated in cold diethyl ether until all monomers were removed.

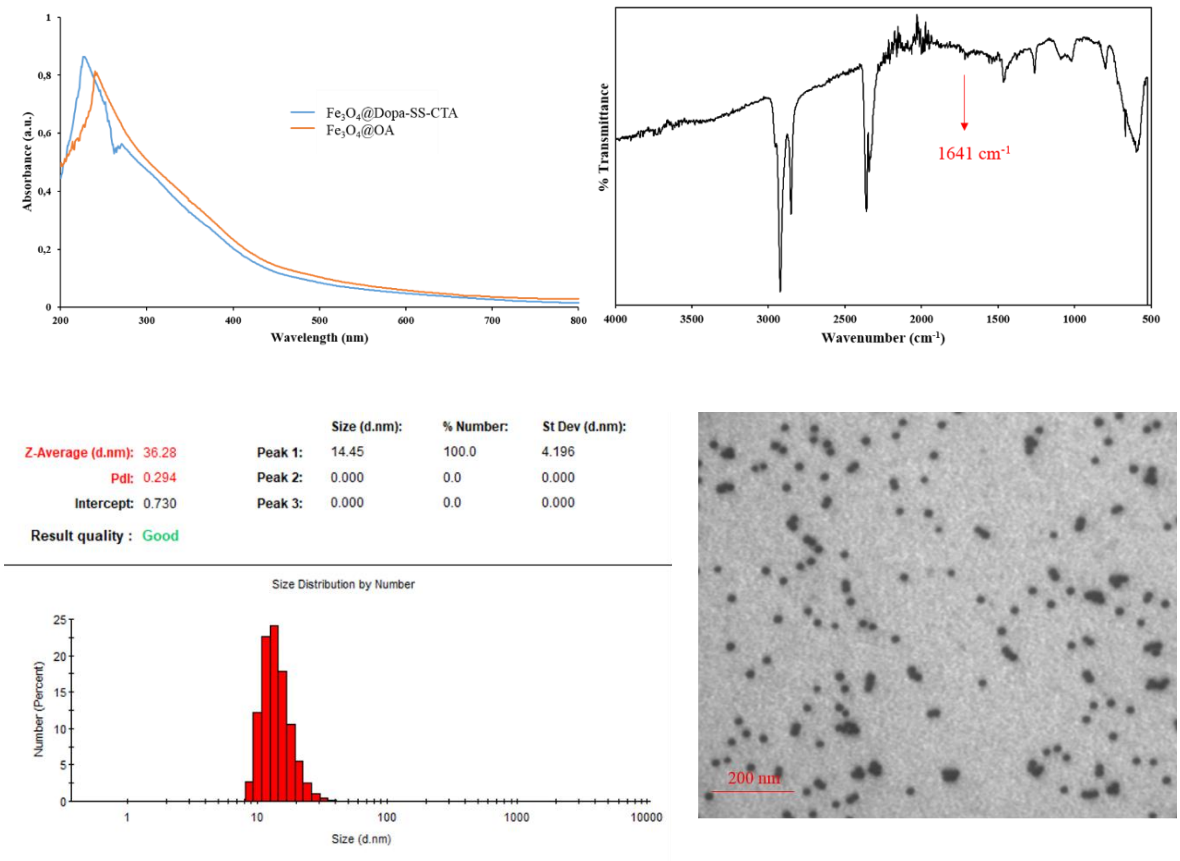

Figure 4.14. UV spectroscopy (top left), FT-IR spectrum (top right), DLS analysis (bottom left) and TEM image (bottom right) of Fe_3O_4@Dopa-SS-CTA.

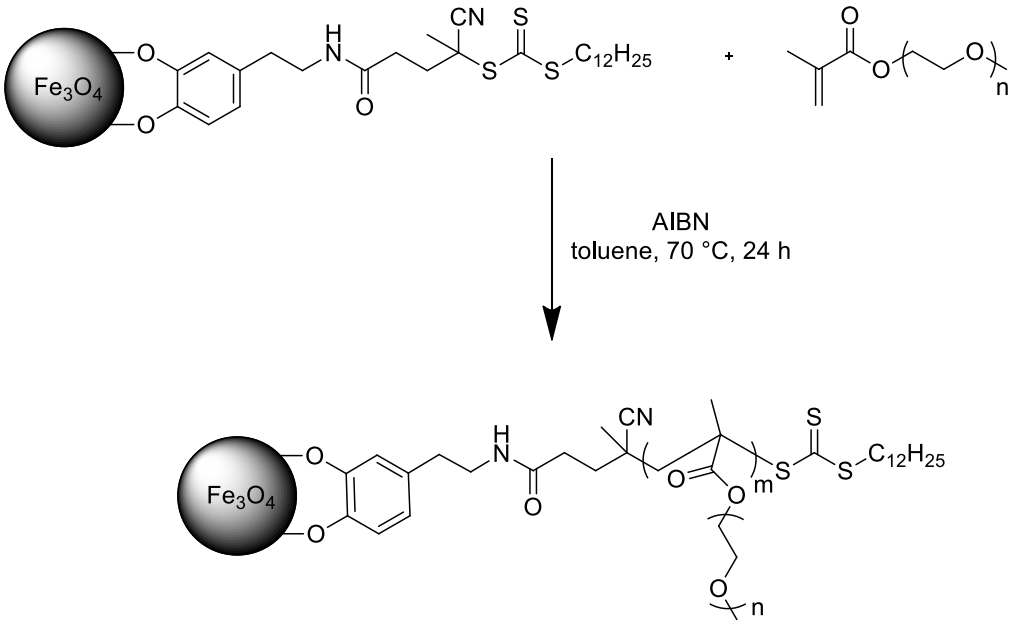

Figure 4.15. Surface initiated RAFT polymerization of PEGMEMA.

Characterization of surface initiated polymers was carried out with FT-IR, UV spectroscopy, TEM and DLS. From FT-IR results, the peak at 1725 cm^{-1} comes from the carbonyl groups of PEGMEMA. The peak at 1100 cm^{-1} comes from the C-O-C ether stretch. These peaks show that successfully grown polymers from the surface of iron oxide nanoparticles. In UV spectroscopy, the peak at 308 nm that corresponds to trithiocarbonate group shows the formation of polymers (Figure 4.16). From DLS results, the diameter of polymer-coated iron oxide nanoparticles was calculated as 22.3 nm.

After the polymerization of PEGMEMA from the surface of iron oxide nanoparticles, Fe_3O_4@PEGMEMA molecules were dispersible in water even though Fe_3O_4@Dopa-CTA molecules were not dispersible in water (Figure 4.17). Because of the presence of hydrophilic p(PEGMEMA) polymers on the nanoparticle surface, these become dispersible in aqueous media.

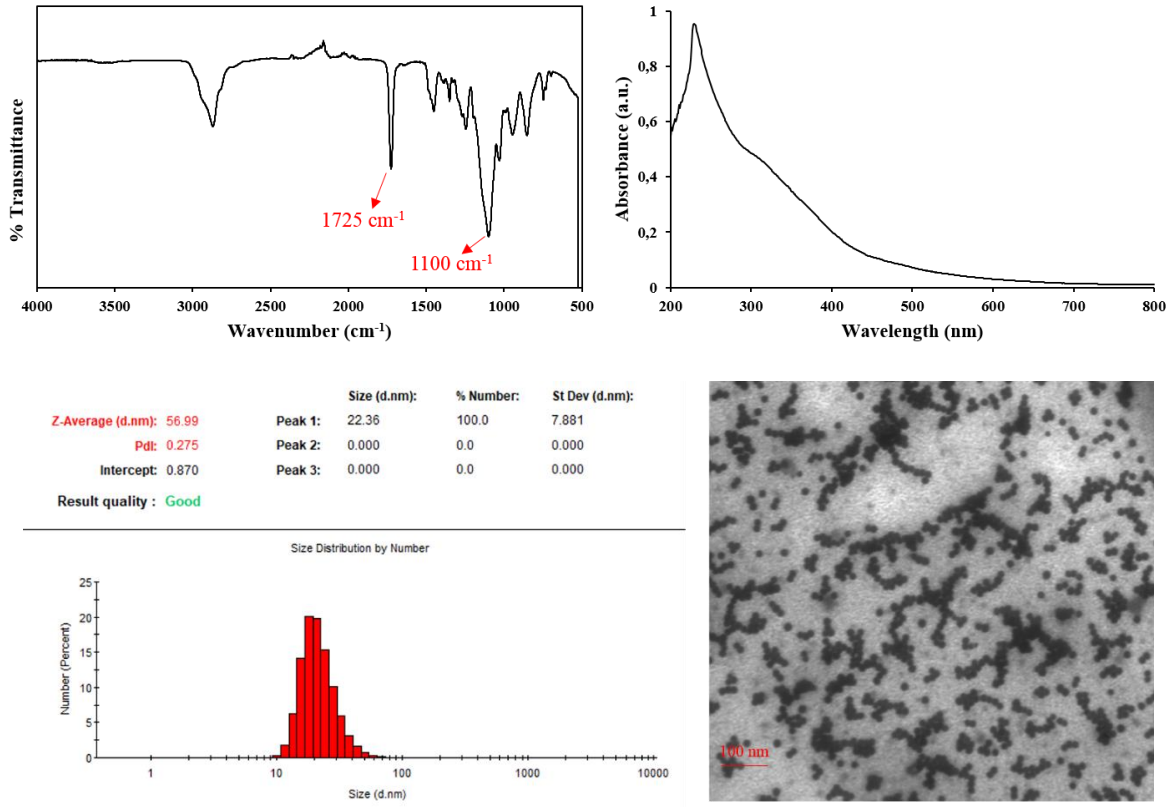

Figure 4.16. FT-IR spectrum (top left) and UV-Vis spectroscopy (top right), DLS analysis (bottom left) and TEM image (bottom right) of Fe_3O_4@Dopa-PEGMEMA.

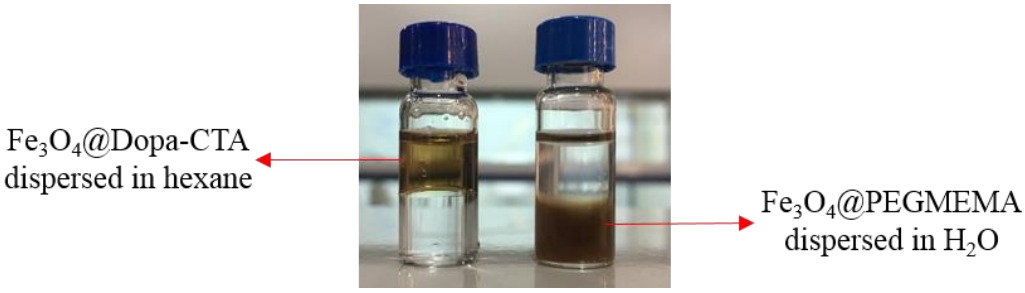

Figure 4.17. Dispersibility difference of Fe_3O_4@Dopa-CTA (left) and Fe_3O_4@PEGMEMA nanoparticles.

4.11. Surface Initiated RAFT Polymerization of PEGMEMA (Fe_3O_4@Dopa-SS-PEGMEMA)

After successful conjugation of dopamine modified CTA to iron oxide nanoparticles, RAFT polymerization of PEGMEMA was done by grafting-from method in the presence of AIBN and toluene (Figure 4.18). The reaction mixture was purged with N_2 for 20 minutes. Then, it was stirred at 75 °C for 8, 16 and 24 hours to see the molecular weight difference upon increase in time. After the polymerization reaction, black viscous liquid was precipitated in cold diethyl ether until removal of unreacted monomers. The characterization of grafted polymers was achieved using UV spectroscopy, DLS, TEM and FT-IR spectrum shown in Figure 4.19. The peak at 1725 cm^{-1} originates from the carbonyl groups of PEGMEMA and the peak at 1100 cm^{-1} belongs to the ether groups of the polymers. In addition, the peak at 320 nm in UV spectroscopy indicates the presence of the trithiocarbonate groups at the chain end of the polymers. These indications combined demonstrate that polymerization reaction occurred successfully. As a physical observation, a small piece of polymer-coated iron oxide nanoparticles was added into water. It was observed that it was dispersible in water, whereas the initial CTA immobilized iron oxide nanoparticles were not dispersible in water. According to DLS results, Fe_3O_4@Dopa-SS-PEGMEMA molecule possessed a diameter of 55 nm.

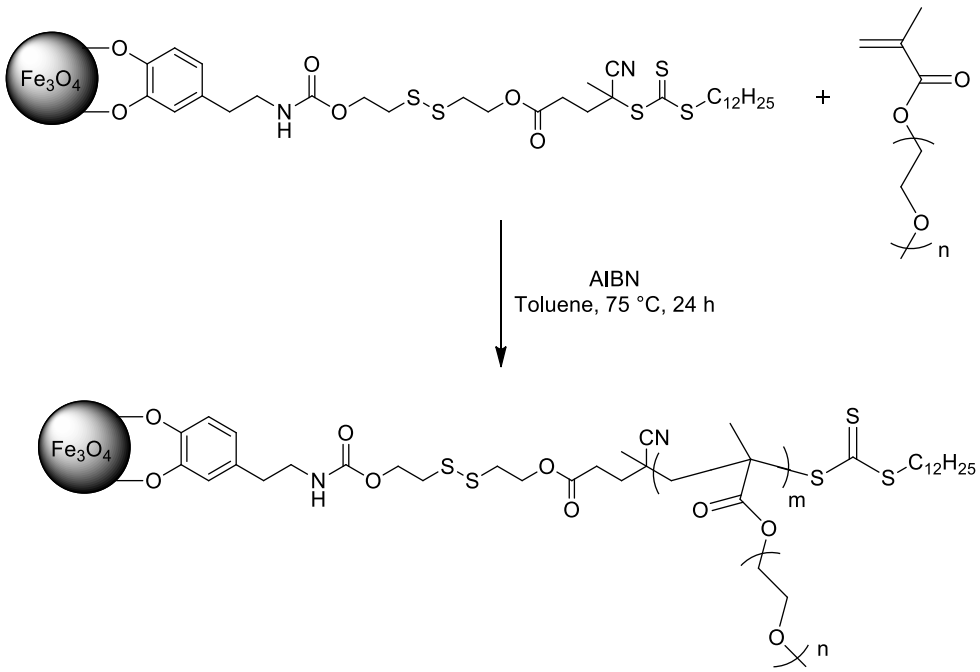

Figure 4.18. Synthesis of Fe_3O_4@Dopa-SS-PEGMEMA by RAFT polymerization.

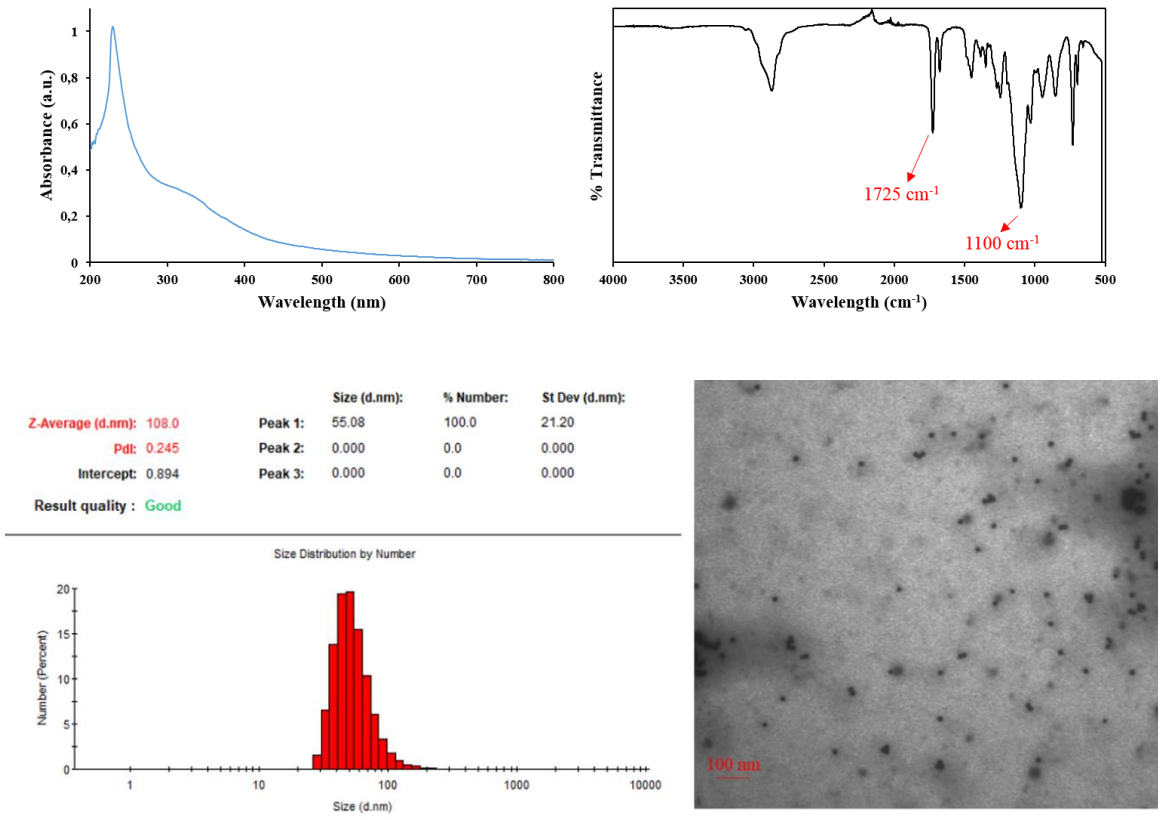

Figure 4.19. UV spectroscopy (top left) FT-IR spectrum (top right), DLS analysis (bottom left) and TEM image (bottom right) of Fe_3O_4@Dopa-SS-PEGMEMA.

4.12. Separation of Iron Oxide Nanoparticles and PEGMEMA

When polymers are grown from the surface of iron oxide nanoparticles, their molecular weights and polydispersity indexes cannot be calculated. However, the system that were created in this project enables us to separate iron oxide nanoparticles and polymers so that their molecular weights and PDI values van be calculated. Because disulfide group between nanoparticles and polymers can be broken by thiol containing materials. For this reason, DTT was used to do so. Polymer-coated iron oxide nanoparticles and DTT were dissolved in phosphate buffer solution and stirred at room temperature for 1 hour (Figure 4.20). Then, polymers and nanoparticles were centrifuged to separate from each other by solubility difference. Iron oxide nanoparticles without PEG polymers are not dispersible in water. Since the polymers are PEG based, they are hydrophilic and soluble in water. This is shown in Figure 4.21. Characterization of these separated molecules was done with Ellman's analysis. As a physical observation, when Ellman's analysis was done on cleaved iron oxide nanoparticles and polymers, the color of the solution turned into yellow. That was a positive test for this analysis. In addition, in UV-Vis spectroscopy, expected peak at 412 nm was observed for both nanoparticles and polymers (Figure 4.22). This proved that nanoparticles and polymers have thiol group in their backbones. Ellman analysis was also applied to Fe_3O_4@Dopa-SS-PEGMEMA molecule as the control group. There was no peak at 412 nm in UV spectroscopy. This was expected since there was no free thiol group in the molecule.

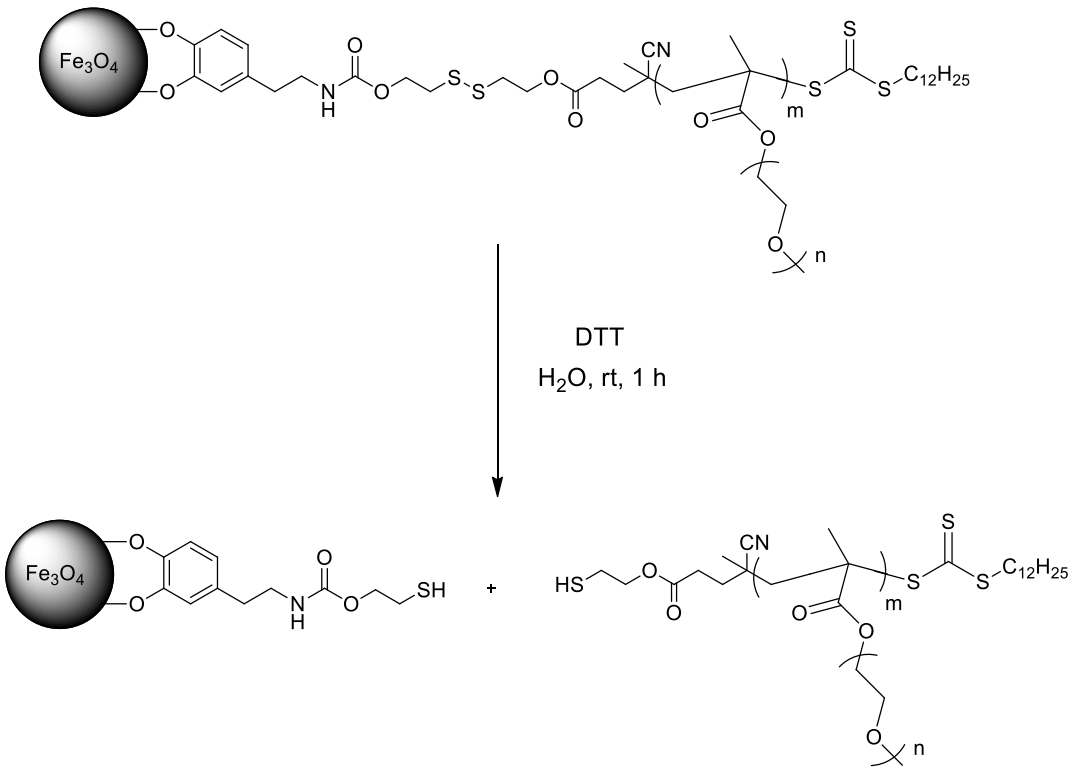

Figure 4.20. Cleavage of disulfide bond in polymer-coated nanoparticles by DTT.

Figure 4.21. Dispersibility of Fe_3O_4@Dopa-SS-PEGMEMA in water (left), after treatment with DTT and centrifugation.

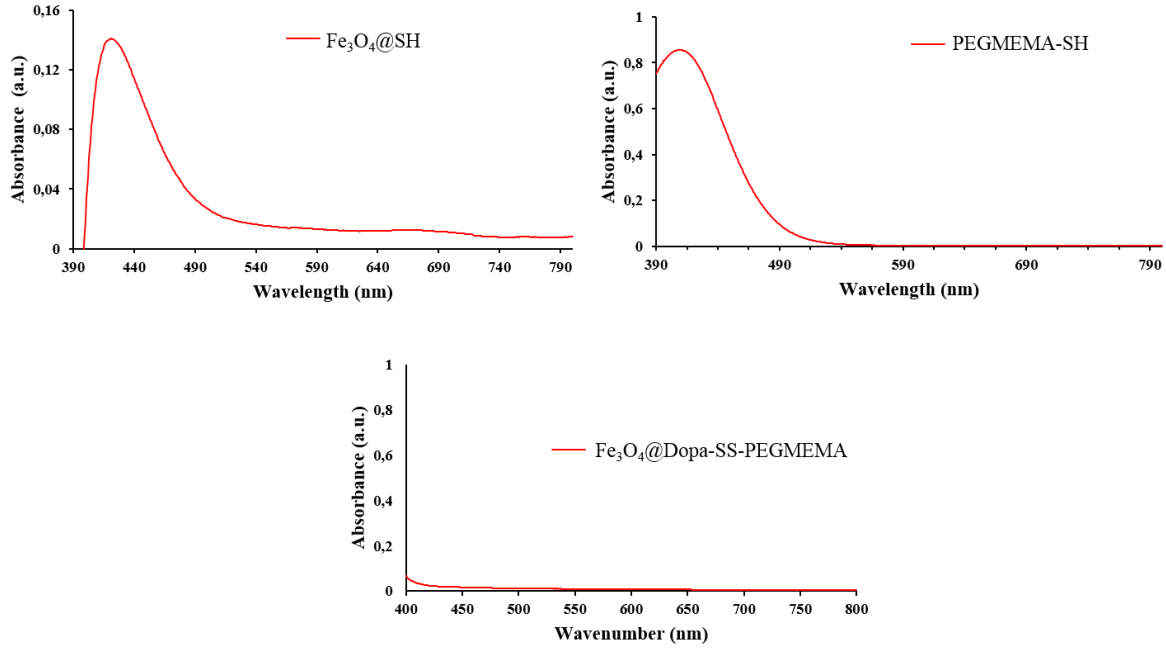

Figure 4.22. UV-Vis spectra of cleaved iron oxide nanoparticles (upper-left), PEGMEMA (upper-right) and Fe_3O_4@Dopa-SS-PEGMEMA (without DTT exposure) upon treatment with Ellman's reagent.

4.12.1. Molecular Weight and PDI Analysis of Grafted Polymers

The molecular weights of the polymers that were cleaved from the surface of iron oxide nanoparticles were analyzed by gel permeation chromatography (GPC) (Table 1). Polymerization reaction was set up for 8, 16, 24 hours under the same conditions to determine how molecular weights were changing with time.

Table 4.1. Molecular weights and PDI values of polymer-coated iron oxide nanoparticles having different time polymerizations.

Polymer-Coated Iron Oxide Nanoparticles	Different Trials of polymerization/cleavage	Molecular Weight of cleaved polymers	Polydispersity Index (PDI)
Fe_3O_4@Dopa-SS-PEGMEMA (8 h)	Polymerization 1	48 kDa	1.73
	Polymerization 2	59 kDa	1.65
	Polymerization 3	55 kDa	1.68
Fe_3O_4@Dopa-SS-PEGMEMA (16 h)	Polymerization 1	58 kDa	1.60
	Polymerization 2	59 kDa	1.60
	Polymerization 3	51 kDa	1.77
Fe_3O_4@Dopa-SS-PEGMEMA (24 h)	Polymerization 1	54 kDa	1.75
	Polymerization 2	59 kDa	2.20
	Polymerization 3	55 kDa	1.32

According to GPC results, it was clearly seen that molecular weights of 8, 16 and 24 hour polymers were close to one another. Therefore, the polymerization reactions that will be done in future of this project will take 8 hours since it is enough to reach desired molecular weights.

4.13. Conclusion

In this project, a novel water dispersible polyethylene glycol based two types of iron oxide nanoparticles were synthesized by surface-initiated RAFT polymerization. One type of polymer-coated iron oxide nanoparticles had disulfide bond between iron oxide and polymers. The other type lacked the disulfide bond. For the creation of such polymer brushes, monodisperse iron oxide nanoparticles were synthesized by thermal decomposition method. Polymerization with PEGMEMA was achieved to provide water dispersibility using the grafting-from approach. Disulfide containing polymer-coated iron oxide nanoparticles were cleaved to release the surface bound polymers using a reducing agent. This also enabled determination of the molecular weights and PDI values of the grafted polymers.

In the future, polymerization reactions with different polymerization durations and amount of monomers will be investigated to observe the changes in molecular weights. The end groups of these polymers are trithiocarbonate groups that can be replaced by using functional azo initiator. For this reason, NHS activated carboxylic acid bearing azo initiator was synthesized and it will be used for the modification of these surface grafted copolymers by radical exchange reaction. Using thus introduced reactive groups on the chain end of the polymer coated nanoparticles can be tailored for various applications.

5. FABRICATION OF POLYMER COATED MAGNETIC NANOPARTICLES FOR REVERSIBLE AND NON-REVERSIBLE CONJUGATIONS

5.1. Aim of the Study

The aim of this study is to produce polymer-coated magnetic nanoparticles that are dispersible in water and having reactive functional groups in their structures. These magnetic and polymer-coated magnetic nanoparticles will be used for biomedical applications. These polymers can be grown from the surface of nanoparticles, which is called grafting-from method. Or they can be synthesized and then they are attached to nanoparticles, which is called grafting-to method. In order to immobilize these polymers onto the surface of nanoparticles, anchoring groups attached to the polymers are needed.

In this study, dopamine was used as the anchoring group. Once the chain transfer agent having dopamine group was immobilized on top of the nanoparticles, polymers were grown from the iron oxide nanoparticle surfaces by using RAFT polymerization method. PEGMEMA monomers were used for this polymerization. After synthesizing polymer-coated iron oxide nanoparticles, end groups of polymers were modified by using radical cross coupling reaction. Thus obtained polymer coated iron oxide nanoparticles were decorated with NHS activated carboxylic acid and pyridyl disulfide reactive groups. The presence of these functional groups were confirmed using amine and thiol-containing fluorescent dyes. Functionalized iron oxide nanoparticles can react with amine containing peptide, cRGDfK which is a targeting group for cancer cells. Furthermore, using the disulfide exchange reaction they can react with thiol containing anti-cancer therapeutic agents which will be released in presence of glutathione to selectively kill the cancer cells.

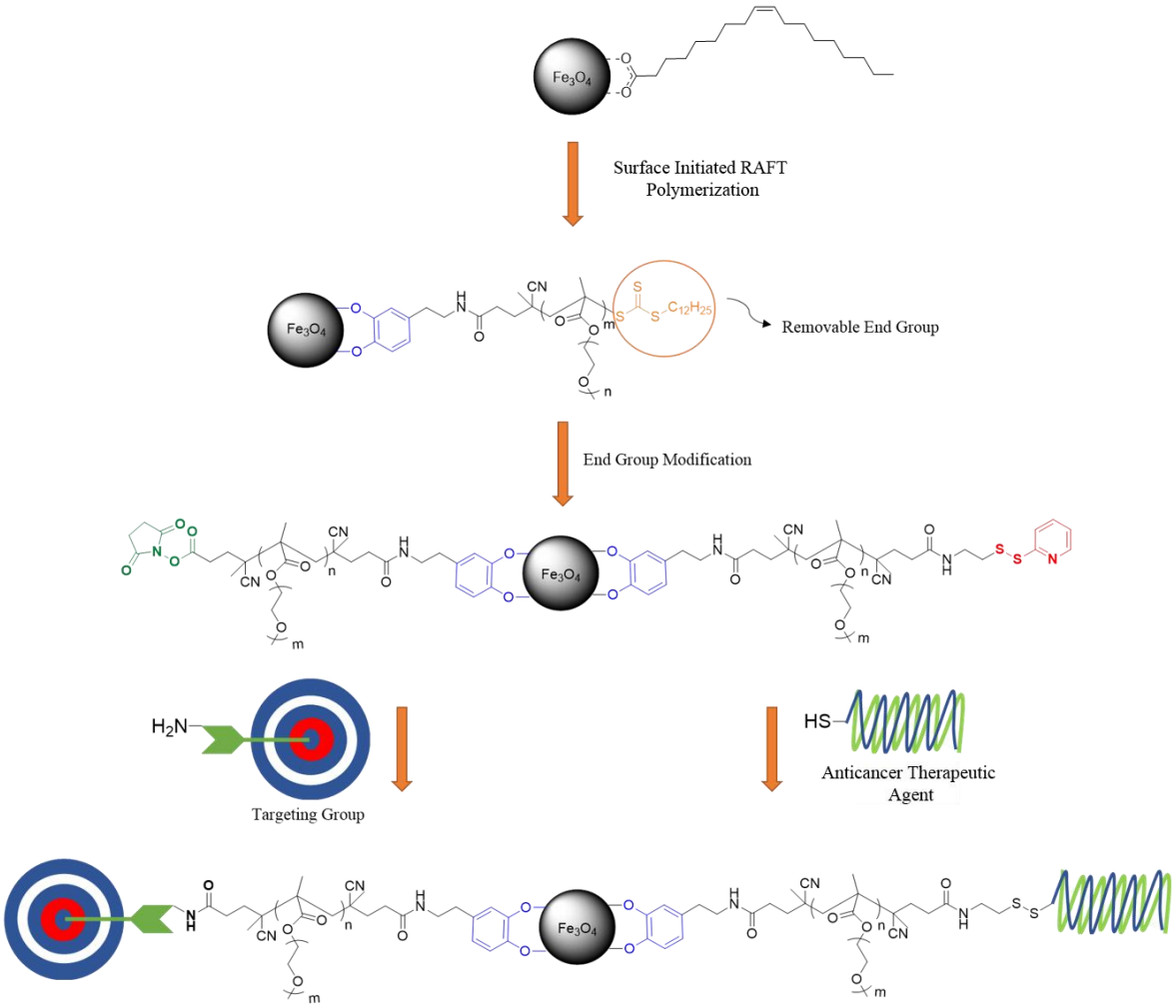

Figure 5.1. General scope of the project.

6. EXPERIMENTAL

6.1. Synthesis of 2-(pyridin-2-yldisulfanyl)ethanaminium

This thiol disulfide exchange reaction took place between aldrithiol and cysteamine. The synthesis of this reaction was taken from the literature.[73] Aldrithiol (830 mg, 3.68 mmol) was dissolved in 3 mL of MeOH. Then, cysteamine (286 mg, 2.52 mmol) was dissolved in 2 mL of methanol and added to the previous solution. Then, it was allowed to stir at room temperature for 5 hours to give desired compound. After the reaction was complete, reaction mixture was added to cold diethyl ether dropwise. White solid was precipitated and collected by filtration method (402 mg, 49 % yield).

6.2. Synthesis of (E)-4,4'-(diazene-1,2-diyl)bis(4-cyano-N-(2-(pyridin-2-yldisulfanyl) ethyl) entanamide) (PdS-ACVA)

This compound was synthesized according to the literature.[74] For this synthesis, 2-(pyridin-2-yldisulfanyl) ethanaminium (1.25g, 5.63 mmol), V501 (658 mg, 2.35 mmol) and TEA (595 mg, 5.88 mmol) were dissolved in 5 mL of $CHCl_3$. Then, EDCI which was dissolved in 5 mL of chloroform was dropped into this mixture at 0 ^{o}C for 1 hour. After that, final mixture was allowed to stir at room temperature for 24 hours. In order to purify the obtained product, the solution was extracted with 10 mL of distilled water 2 times. Then, organic and aqueous part were separated from each other by separatory funnel. After that, organic part was extracted with 10 mL of 0.1 M HCl and saturated $NaHCO_3$ 2 times, respectively. Then, Na_2SO_4 was added to remove the water in the solution. Finally, the solvent was removed by rotary evaporation. The obtained product was purified by column chromatography using ethyl acetate/ hexane (4:1) (888 mg, 51% yield). ^{1}H NMR ($CDCl_3$) δ (ppm): 8.51 (d, 2H), 7.61 (t, 2H), 7.55 (s, 2H), 7.51 (d, 2H), 7.16 (t, 2H), 3.46-3.63 (m, 4H), 2.92 (t, 2H), 2.90 (t, 2H), 2.20-2.55 (m, 8H), 1.70 (s, 6H).

6.3. End Group Modifications of Polymer-Coated Fe_3O_4 Nanoparticles

6.3.1. End Group Modification with Pyridyl Disulfide Containing Azo Initiator (Fe_3O_4@PEGMEMA@ PDS)

Pyridyl disulfide functionalized V501 azo initiator (PDS-ACVA) (12.4 mg, 0.02 mmol) and polymer-coated Fe_3O_4 nanoparticles (50 mg) were dissolved in 2 mL of DMF. Then, the mixture was purged with N_2 for 20 minutes. After that, it was allowed to stir at 70 ^oC for 16 hours. When the reaction was complete, to get the obtained product, it was dialyzed against 200 mL of acetonitrile using dialysis membrane (molecular weight cutoff 3500 Da) for 36 hours. Finally, the solvent was removed by rotary evaporation.

6.3.2. End Group Modification with NHS activated Carboxylic Acid Containing Azo Initiator (Fe_3O_4@PEGMEMA@ NHS)

NHS-activated Carboxylic Acid functionalized V501 azo initiator (NHS-ACVA) (9.5 mg, 0.02 mmol) and polymer-coated Fe_3O_4 nanoparticles (50 mg) were dissolved in 2 mL of DMF. Then, the mixture was purged with N_2 for 20 minutes. After that, it was allowed to stir at 70 ^{o} C for 16 hours. As the purification part, the reaction mixture was dialyzed against 200 mL of acetonitrile using dialysis membrane (molecular weight cutoff 3500 Da) for 36 hours. Finally, the solvent was removed by rotary evaporation.

6.3.3. End Group Modification with NHS activated Carboxylic Acid + Pyridyl Disulfide Containing Azo Initiator (Fe_3O_4@PEGMEMA@PdS+NHS)

NHS activated carboxylic acid functionalized V501 azo initiator (NHS-ACVA) (1.9 mg, 4 µmol) and pyridyl disulfide functionalized V501 azo initiator (PDS-ACVA) (11 mg, 16 µmol) and polymer-coated Fe_3O_4 nanoparticles (50 mg) were dissolved in 2 mL of DMF. Then, the mixture was purged with N_2 for 20 minutes. After that, it was allowed to stir at 70 ^{o} C for 16 hours. As the purification part, the reaction mixture was dialyzed against 200 mL

of acetonitrile using dialysis membrane (molecular weight cutoff 3500 Da) for 36 hours. Finally, the solvent was removed by rotary evaporation.

6.4. Modification of Polymer-Coated Fe_3O_4 Nanoparticles with Glutathione

This compound was obtained by disulfide exchange reaction between Fe_3O_4@PEGMEMA@PDS and glutathione. Fe_3O_4@PEGMEMA@PDS (15 mg) and glutathione (3.07 mg, 10 mmol) were dissolved in H_2O. Then, TEA (1.01 mg, 10 mmol) was added to this solution. The reaction mixture was stirred at room temperature for 24 hours. After the reaction, the reaction mixture was dialyzed against 200 mL of water using dialysis membrane (molecular weight cutoff 3500 Da) for 24 hours. Finally, the solvent was removed by rotary evaporation to get desired compound.

6.5. Fluorescent Dye Attachment to Functionalized Polymer-Coated Fe_3O_4 Nanoparticles

6.5.1. Fluorescent Dye Attachment to Pyridyl Disulfide Functionalized Fe_3O_4 Nanoparticles by Disulfide Exchange Reaction

For this reaction, Fe_3O_4@PEGMEMA@PDS (10 mg) and BODIPY-SH (0.1 mg, 0.2 µmol) were dissolved in 200 µl of THF. Then, TEA (21 µg, 0.2 µmol) was added to the solution. The mixture was stirred at room temperature for 24 hours. After the conjugation of BODIPY-SH, the mixture was dropped into cold diethyl ether to get rid of unreacted dye molecules. Finally, dye containing polymer-coated Fe_3O_4 nanoparticles were obtained by centrifugation method.

6.5.2. Fluorescent Dye Attachment to NHS Activated Carboxylic Acid Functionalized Fe_3O_4 Nanoparticles by Amidation Reaction

For this reaction, Fe_3O_4@PEGMEMA@NHS (10 mg) and Fluorescein-NH_2 (0.28 mg, 0.8 µmol) were dissolved in 200 µl of dry DMF. Then, TEA (0.16 mg, 1.6 µmol) was added to the solution. The mixture was stirred at room temperature for 24 hours. After the reaction, the reaction mixture was dialyzed against 200 mL of acetonitrile using dialysis membrane (molecular weight cutoff 3500 Da) for 24 hours. Finally, the solvent was removed by rotary evaporation to get dye containing polymer-coated Fe_3O_4 nanoparticles.

6.6. cRGDfK and 1-amino-2-propanol Attachment to NHS Activated Carboxylic Acid + Pyridyl Disulfide Functionalized Polymer-Coated Fe_3O_4 Nanoparticles

6.6.1. cRGDfK Attachment to NHS Activated Carboxylic Acid and Pyridyl Disulfide Functionalized Polymer-Coated Fe_3O_4 Nanoparticles

For the targeting group and apoptotic peptide attachment to Fe_3O_4 nanoparticles, first conjugation was done by amidation reaction between NHS activated carboxylic acid of the nanoparticles and amine group of cRGDfK. Fe_3O_4@PEGMEMA@NHS+PdS (20 mg) and cRGDfK (0.1 mg, 0.72 µmol) were dissolved in 200 µL of dry DMF. Then, this mixture was stirred at room temperature for 24 hours under N_2. After the reaction, in order to remove unreacted cRGDfK, the mixture was dialyzed against 400 mL of water using dialysis membrane (molecular weight cutoff 3500 Da) for 24 hours.

6.6.2. 1-amino-2-propanol Attachment to NHS Activated Carboxylic Acid and Pyridyl Disulfide Functionalized Polymer-Coated Fe_3O_4 Nanoparticles

In order to remove the unreacted NHS groups in the cRGDfK attached Fe_3O_4 nanoparticles, 1-amino-2-propanol (0.23 mg, 3.04 µmol) was added to Fe_3O_4 nanoparticles (19 mg) in 500 µL of DCM. It was stirred at room temperature for 24 hours. After the

reaction, the mixture was dropped into cold diethyl ether to remove unreacted 1-amino-2-propanol. Finally, the solvent was removed by rotary evaporation.

7. RESULTS AND DISCUSSIONS

7.1. Synthesis of Pyridyl Disulfide Functionalized V-501 Azo Initiator (PDS-ACVA)

The aim of synthesizing this material is to enable the end group modification of the surface initiated polymers using a thiol-disulfide exchange reaction. The end groups of the polymers grafted-from the nanoparticle surfaces contain trithiocarbonate groups. These groups can be replaced by desired functional groups using azo-initiators under radical exchange reaction conditions. The synthesis of pyridyl disulfide (PDS) containing azo initiator involves two steps. 2-(pyridin-2-yldisulfanyl) ethanaminium was synthesized from aldrithiol and cysteamine in the presence of acetic acid and methanol as the solvent according to literature procedures.[73] Thus obtained 2-(pyridin-2-yldisulfanyl) ethanaminium was then reacted with V-501 azo initiator with EDCI, TEA, using $CHCl_3$ as the solvent (Figure 7.1). This material was purified by column chromatography on silica gel. The characterization was done with ^1H NMR (Figure 7.2). The peaks at 2.2 - 2.55 ppm come from V-501 and the peaks at 8.51, 7.62, 7.50 ppm come from the pyridine ring. In addition, the peak at 7.56 ppm comes from the amide bond, which shows the successful conjugation.

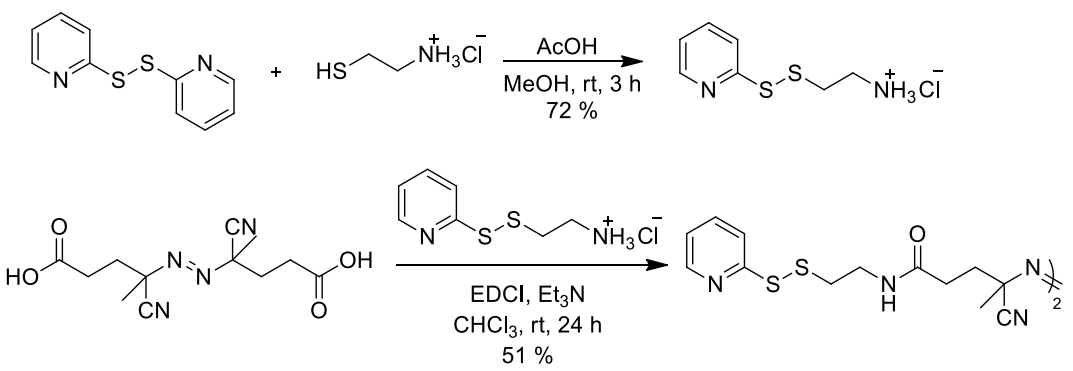

Figure 7.1. Synthetic route of PDS-ACVA azo-initiator.

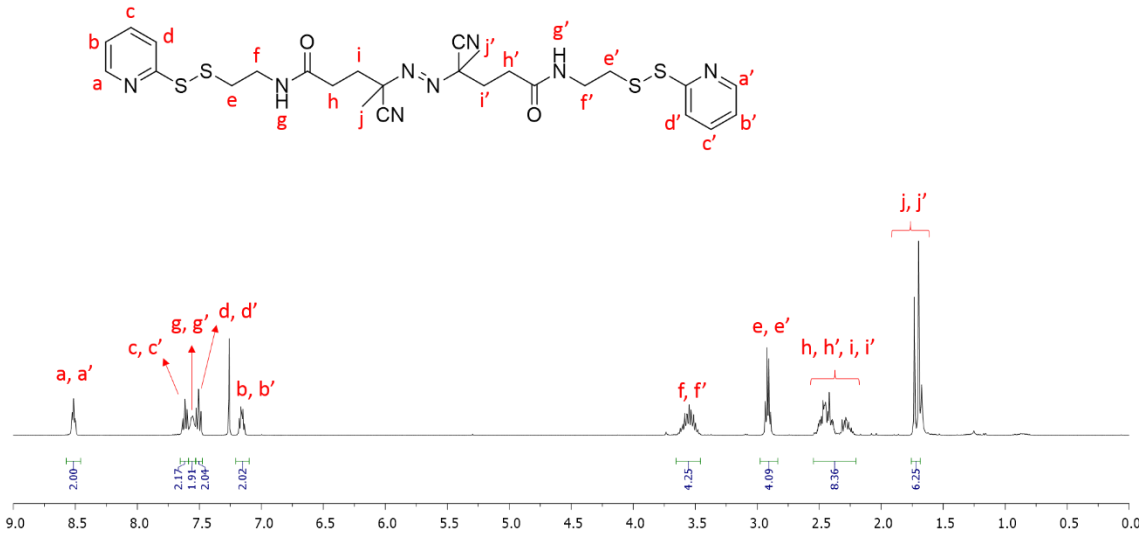

Figure 7.2. ^{1}H NMR spectrum of PDS-ACVA azo-initiator.

7.2. Functionalization of Polymer-Coated Fe_3O_4 Nanoparticles by End Group Modifications

7.2.1. End Group Modification by Pyridyl Disulfide Containing Azo Initiator

Once PEGMEMA was successfully polymerized from the surface of iron oxide nanoparticles, the polymers' end groups were modified by using radical exchange reaction. For this purpose, pyridyl disulfide functionalized V-501 azo initiator was used to replace trithiocarbonate groups of the polymers with pyridyl disulfide groups. Fe_3O_4@PEGMEMA and excess amount of PdS-ACVA were dissolved in dry DMF. Then, reaction mixture was purged with N_2 for 20 minutes to remove O_2 from the reaction environment. After that, the reaction mixture was stirred for 16 hours at 70 °C (Figure 7.3). Once the reaction was complete, the mixture was dialyzed against acetonitrile to get rid of impurities.

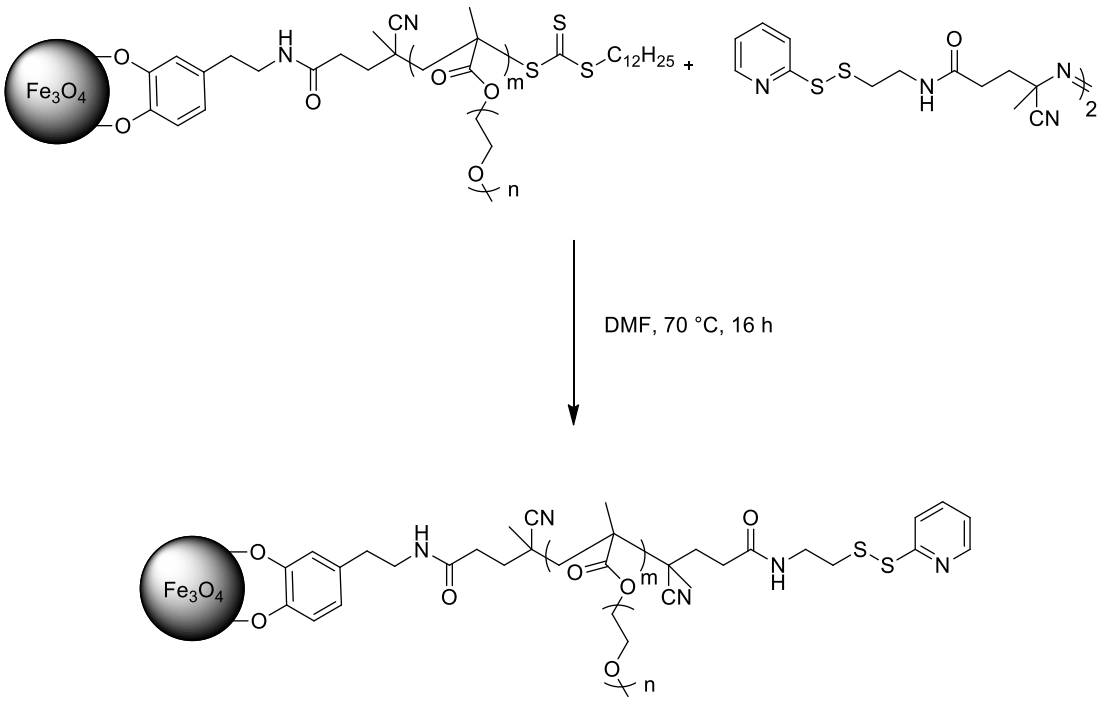

Figure 7.3. End group modification of polymer-coated iron oxide nanoparticles by pyridyl disulfide group.

Characterization of this molecule was carried out with FT-IR and UV-Vis spectroscopy. The characteristic peak at 1575 cm^{-1} in FT-IR and the peak at 290 nm in UV-Vis spectroscopy come from pyridyl disulfide groups (Figure 7.4). In addition, from UV-Vis spectroscopy, it is clearly observable that the peak at 308 nm that corresponds to trithiocarbonate group disappeared and it was replaced by the pyridyl disulfide group. These information proves that the functionalization of polymer coated iron oxide nanoparticles by radical exchange reaction was successful.

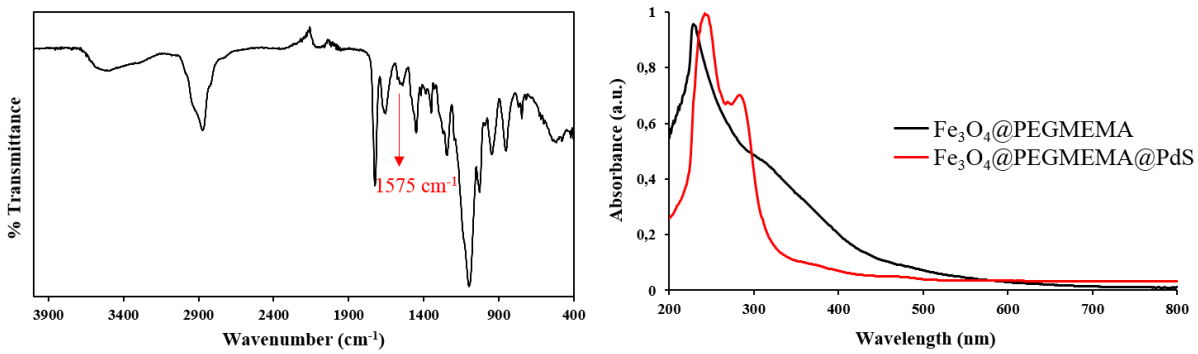

Figure 7.4. FT-IR spectrum (left) and UV-Vis spectroscopy (right) of Fe_3O_4@PEGMEMA@PDS nanoparticles.

7.2.2. End Group Modification by NHS Activated Carboxylic Acid Containing Azo Initiator.

The second functionalization of the end groups of polymer-coated iron oxide nanoparticles was achieved through the introduction of NHS-activated carboxylic acid group using the NHS-activated V-501 azo initiator. The radical exchange reaction took place between Fe_3O_4@PEGMEMA and NHS-ACVA. For this purpose, Fe_3O_4@PEGMEMA and excess amount of NHS-ACVA were dissolved in DMF and the mixture was purged with N_2 for 20 minutes to remove O_2 to prevent the formation of peroxy radicals. Then, the reaction mixture was stirred for 16 hours at 70 °C (Figure 7.5). After the reaction, the mixture was dialyzed against acetonitrile to get rid of impurities.

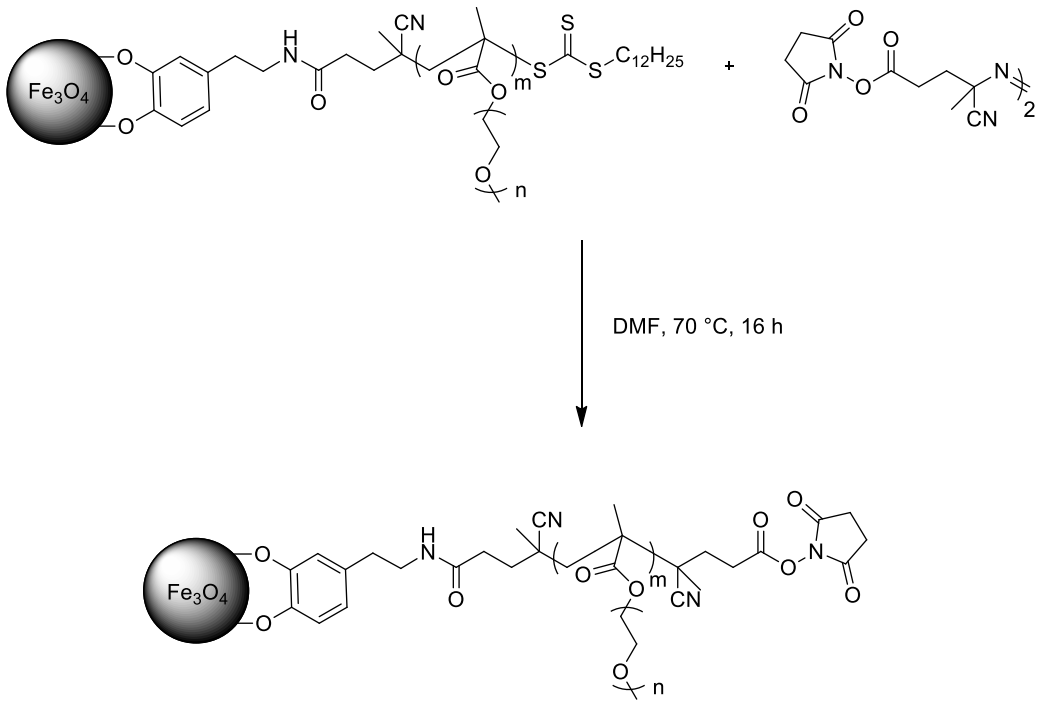

Figure 7.5. End group modification of polymer-coated iron oxide nanoparticles by NHS-activated carboxylic acid group.

Characterization of this transformation was carried out with FT-IR spectroscopy. The characteristic peaks at 1782 and 1812 cm^{-1} in FT-IR originates from the NHS group. In addition, from UV-Vis spectroscopy, it is clearly seen that the peak at 308 nm which corresponds to the trithiocarbonate group disappeared (Figure 7.6). These information proves that the functionalization of polymer coated iron oxide nanoparticles by radical exchange reaction was successful.

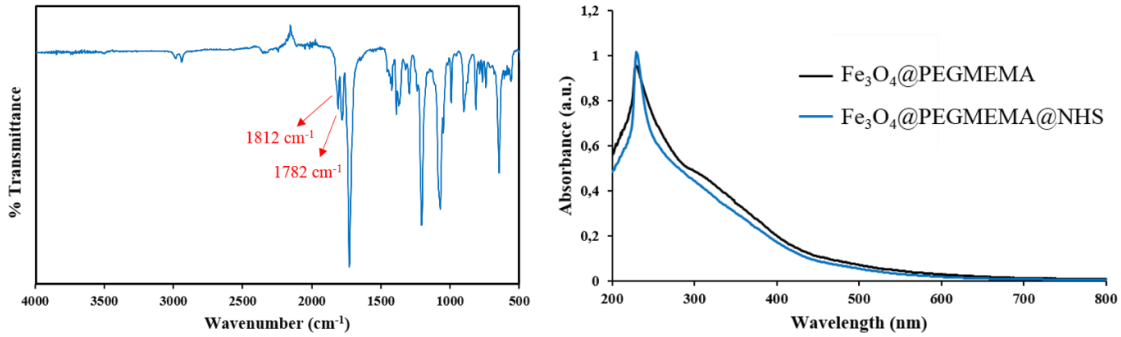

Figure 7.6. FT-IR spectrum (left) and UV-Vis spectra (right) of Fe_3O_4@PEGMEMA@NHS nanoparticles.

7.3. Disulfide Exchange Reaction between Pyridyl Disulfide Functionalized Polymer-Coated Fe_3O_4 Nanoparticles and Glutathione

In order to demonstrate facile functionalization of the pyridyl disulfide functionalized polymer-coated Fe_3O_4 nanoparticles, glutathione (GSH) was used. The disulfide bearing end groups of these nanoparticles are cleaved by thiol bearing molecules such as GSH to give a new disulfide bond after the reaction. To undertake this surface modification, Fe_3O_4@PEGMEMA@PdS and GSH were mixed in water at 37 °C for 1 hour (Figure 7.7).

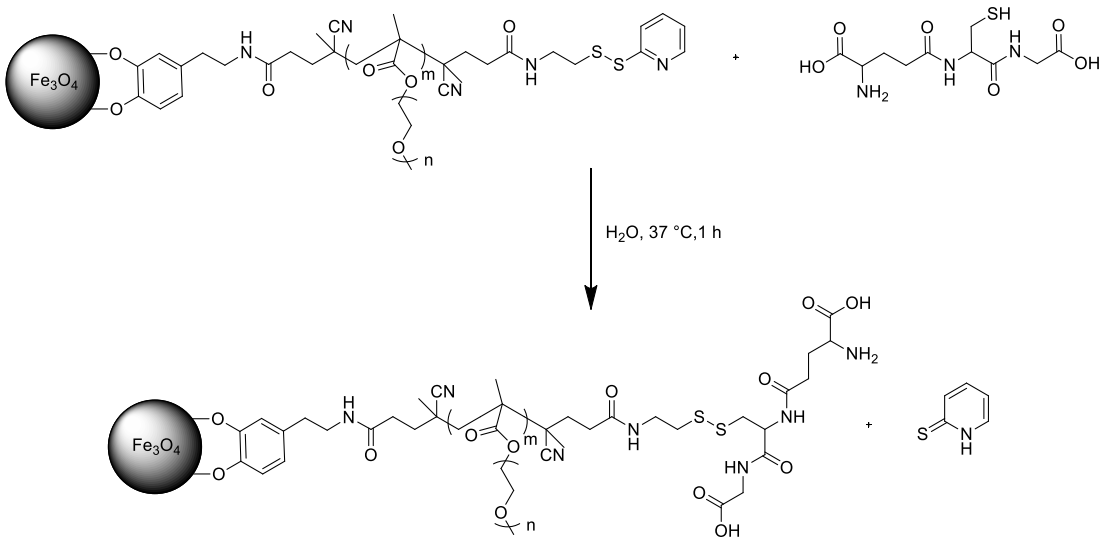

Figure 7.7. Glutathione attachment to Fe_3O_4@PEGMEMA@PDS nanoparticles.

For characterization of this this molecule, UV-Vis spectroscopy was used to observe the release of pyridine-2-thione, by-product of the reaction which gives a peak at 343 nm (Figure 7.8). The characteristic peak corresponds to pyridine-2-thione, which proves the existence of pyridyl disulfide group as the end group of polymer-coated iron oxide nanoparticles, and its release suggests the formation of the new disulfide group.

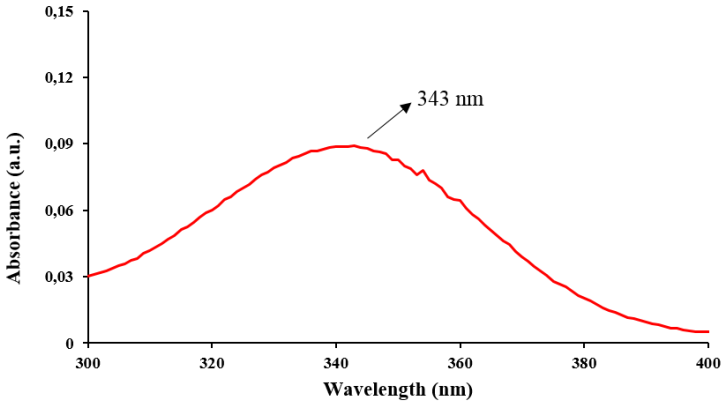

Figure 7.8. UV-Vis spectrum of pyridine-2-thione released from Fe_3O_4@PEGMEMA@PDS nanoparticles.

7.4. Dye Attachment to Pyridyl Disulfide and NHS Activated Carboxylic Acid Functionalized Polymer-Coated Fe_3O_4 Nanoparticles

7.4.1. BODIPY-SH Attachment to Pyridyl Disulfide Functionalized Polymer-Coated Fe_3O_4 Nanoparticles (Fe_3O_4@PEGMEMA@PDS) by Thiol Disulfide Exchange Reaction

Functionalization of Fe_3O_4@PEGMEMA@PdS was investigated by using thiol bearing dye called BODIPY-SH. For this purpose, PDS functionalized polymer-coated magnetic nanoparticles and the thiol bearing dye were mixed in the presence of Et_3N in THF at room temperature for 24 hours (Figure 7.9). At the end of the reaction, the desired dye attached nanoparticles were precipitated in cold diethyl ether, since the dye itself is soluble in ether.

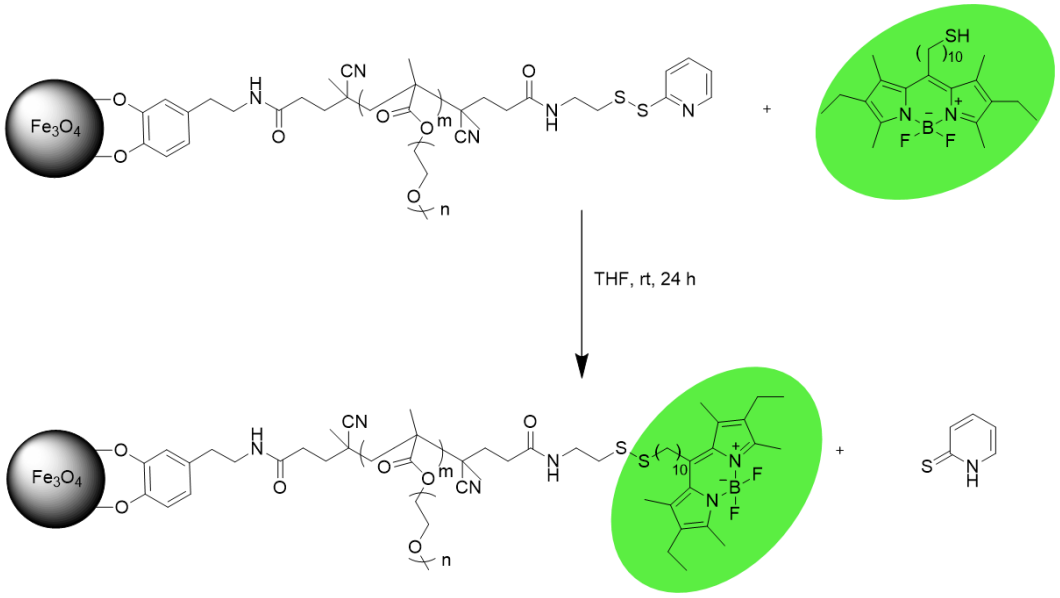

Figure 7.9. BODIPY-SH attachment to Fe_3O_4@PEGMEMA@PDS nanoparticles.

Characterization of dye conjugated nanoparticle was achieved using UV-Vis spectroscopy. The clearly observable peak at 520 nm is characteristic to BODIPY dye. This shows successful conjugation of this dye to Fe_3O_4@PEGMEMA@PDS nanoparticles by disulfide exchange reaction (Figure 7.10). In addition, BODIPY-SH is a hydrophobic dye. After conjugation to the hydrophilic polymer-coated nanoparticles, it becomes a water soluble derivative. In order to visualize this, polymer-coated nanoparticles, BODIPY bearing polymer-coated nanoparticles and free BODIPY-SH were observed under UV light in water and ether phase, respectively (Figure 7.11). As expected, it was observed that the free dye was soluble in ether due to its hydrophobic character. The BODIPY dye bearing polymer-coated nanoparticles were soluble in water since they were grafted with PEG polymers. The transfer of the hydrophobic dye to the aqueous phase illustrates successful conjugation of the dye onto the polymer coated nanoparticle surface.

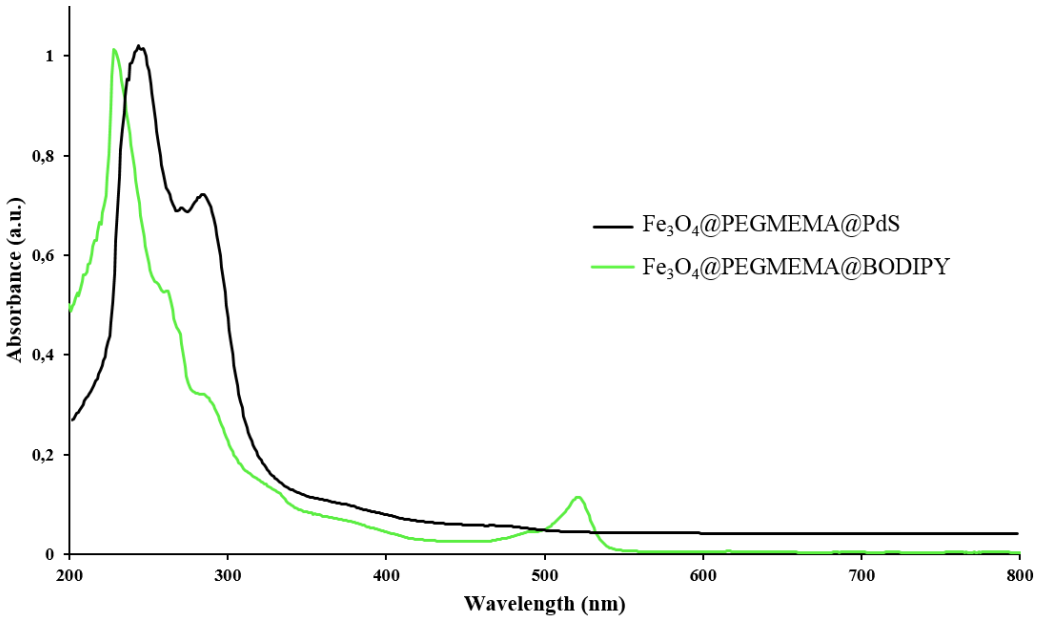

Figure 7.10. UV-Vis spectra of Fe_3O_4@PEGMEMA@PDS and Fe_3O_4@PEGMEMA@BODIPY nanoparticles.

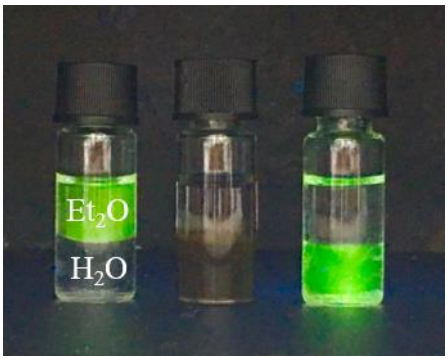

Figure 7.11. Free dye in ether (left), Fe_3O_4@PEGMEMA@PdS in water (middle), BODIPY attached Fe_3O_4@PEGMEMA nanoparticles under UV light.

7.4.2. Fluoresceinamine Attachment to NHS Activated Carboxylic Acid Functionalized Polymer-Coated Fe_3O_4 Nanoparticles (Fe_3O_4@PEGMEMA@NHS) by Amidation Reaction

Functionalization of Fe_3O_4@PEGMEMA@NHS was observed by using a dye that contains amine in its structure. Fe_3O_4@PEGMEMA@NHS and fluoresceinamine were

mixed in the presence of Et_3N in DMF at room temperature for 24 hours (Figure 7.12). At the end of the reaction, the desired compound was dialyzed against water to remove unreacted dye.

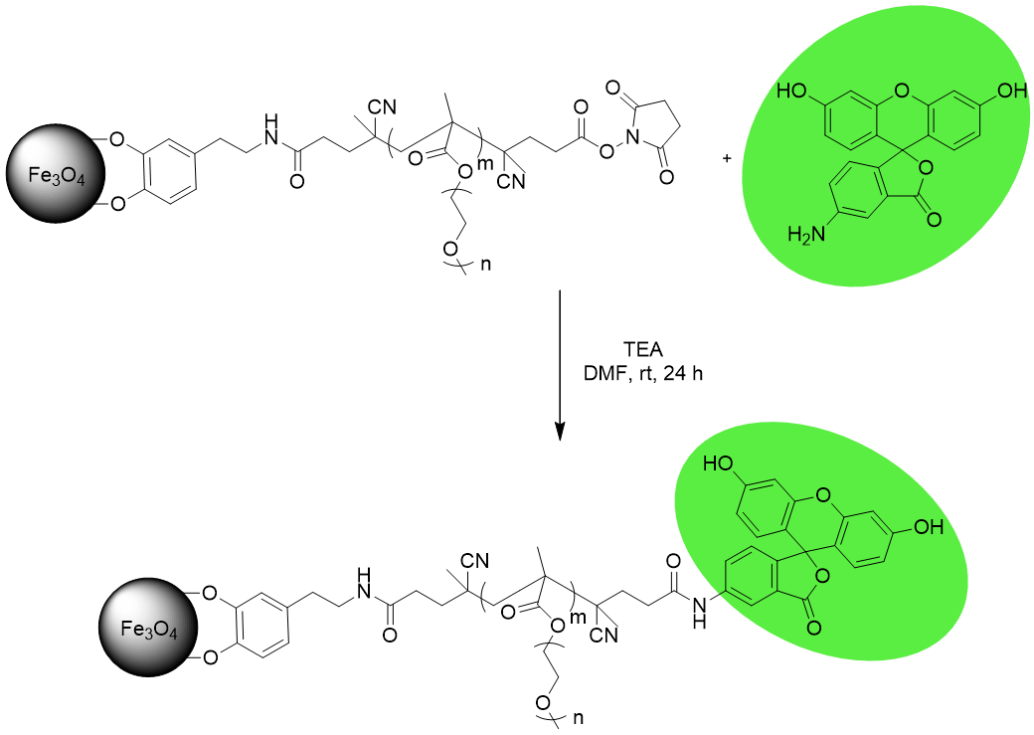

Figure 7.12. Fluoresceinamine attachment to Fe_3O_4@PEGMEMA@NHS nanoparticles.

Characterization of this molecule was achieved by FT-IR and UV-Vis spectroscopy. The peak at 490 nm is characteristic to fluorescein amine. In addition, from FT-IR, it is easily seen that the peaks at 1812 and 1782 cm^{-1} that belong to NHS group disappeared, which proves that NHS groups were replaced by during conjugation of the dye (Figure 7.13). This suggests that conjugation of this dye to Fe_3O_4@PEGMEMA@NHS nanoparticles through amidation reaction was successful.

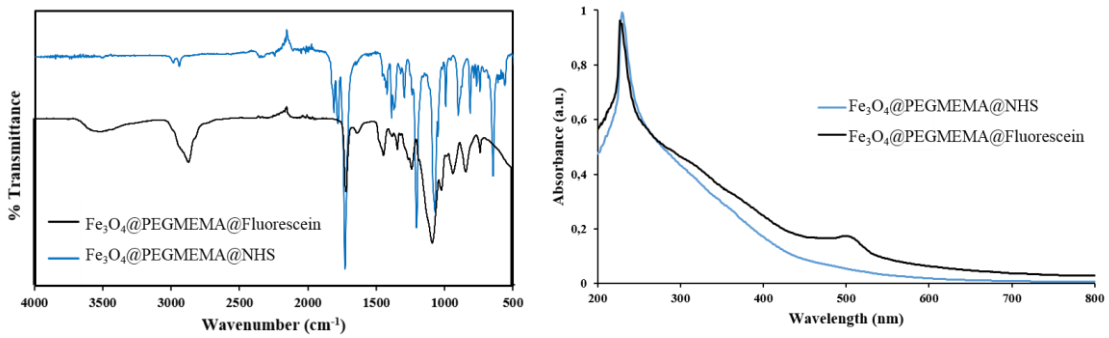

Figure 7.13. FT-IR spectrum (left) and UV-Vis spectra (right) of Fe_3O_4@PEGMEMA@NHS and Fe_3O_4@PEGMEMA@Fluorescein nanoparticles.

7.4. End Group Modification of Polymer-Coated Iron Oxide Nanoparticles by Pyridyl Disulfide and NHS Activated Carboxylic Acid Containing Azo Initiators (Fe_3O_4@PEGMEMA@PDS+NHS)

Once functionalization of both PDS and NHS terminated polymer brushes was investigated by attachment of dyes, these two types of azo initiators were mixed and they were intended to be attached to the polymeric nanoparticles by radical exchange reaction. For this synthesis, Fe_3O_4@PEGMEMA and excess amount of PdS-ACVA and NHS-ACVA were dissolved in dry DMF. Then, reaction mixture was purged with N_2 for 20 minutes to remove O_2. After that, the reaction mixture was stirred for 16 hours at 70 °C (Figure 7.14) Once the reaction was complete, the mixture was dialyzed against acetonitrile to get rid of unreacted azo initiator fragments.

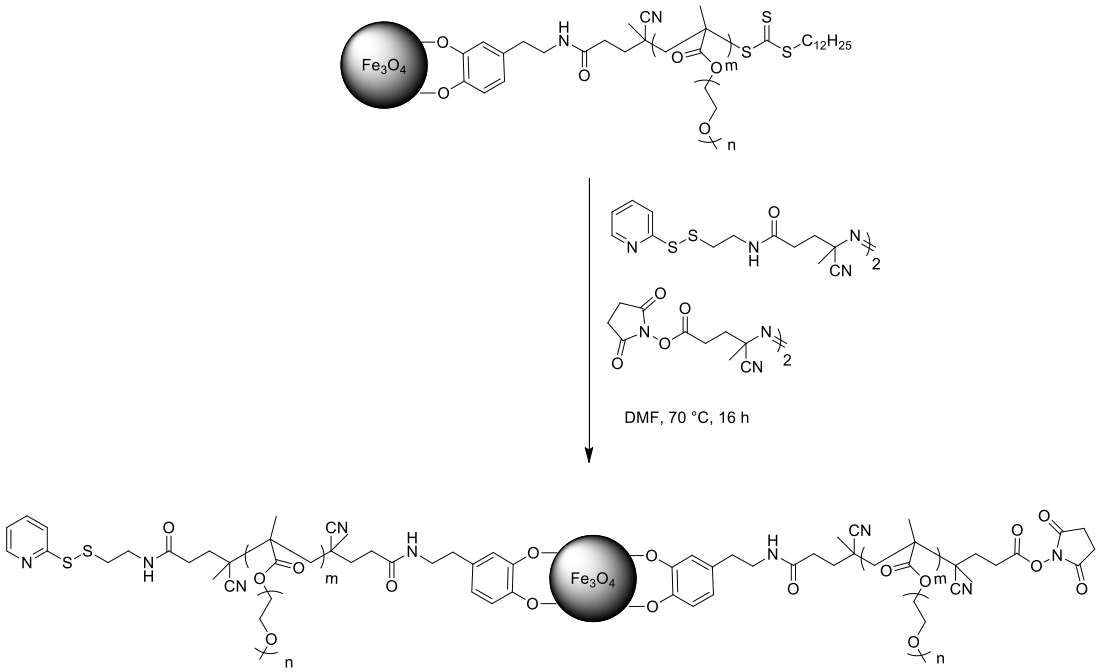

Figure 7.14. End group modification of polymer-coated iron oxide nanoparticles by PDS and NHS functional groups.

Functionalization of this molecule was discussed by successfully attaching thiol and amine functionalized dyes. Characterization of NHS and PDS bearing polymer–coated iron oxide nanoparticles was shown at the beginning of this chapter. After synthesizing this nanoparticles, UV-Vis spectroscopy of it was taken to see if the PDS groups were existing or not. The peak at 280 nm comes from the PDS groups (Figure 7.15). However, NHS group was not seen there since it is not visible in UV-Vis spectroscopy. In order to confirm the NHS availability, cRGDfK which is the targeting group for cancer cells was attached to NHS bearing polymers.

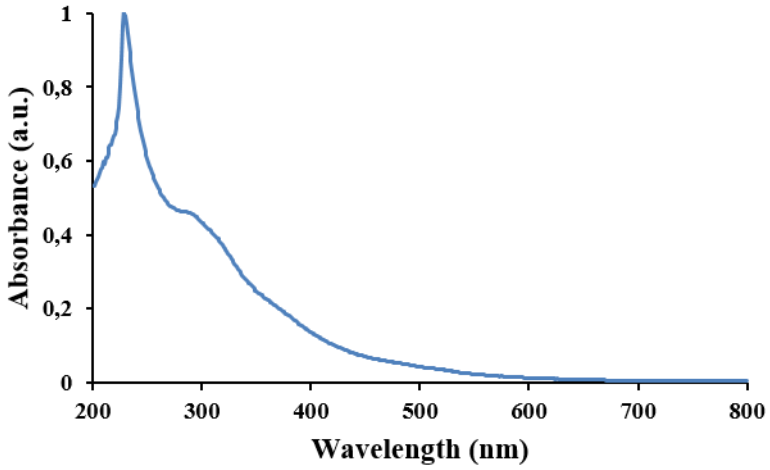

Figure 7.15. UV-Vis spectroscopy of Fe_3O_4@PEGMEMA@PDS+NHS

7.4.1. Attachment of cRGDfK to Fe_3O_4@PEGMEMA@PdS+NHS

After synthesis of Fe_3O_4@PEGMEMA@PdS+NHS, the first peptide which was attached to functionalized iron oxide nanoparticles was cRGDfK which is the targeting group. For this synthesis, Fe_3O_4@PEGMEMA@PdS+NHS and cRGDfK were mixed in dry DMF. The reaction mixture was stirred at room temperature for 24 hours (Figure 7.16). After the reaction was complete, unreacted cRGDfK was removed by dialysis against water.

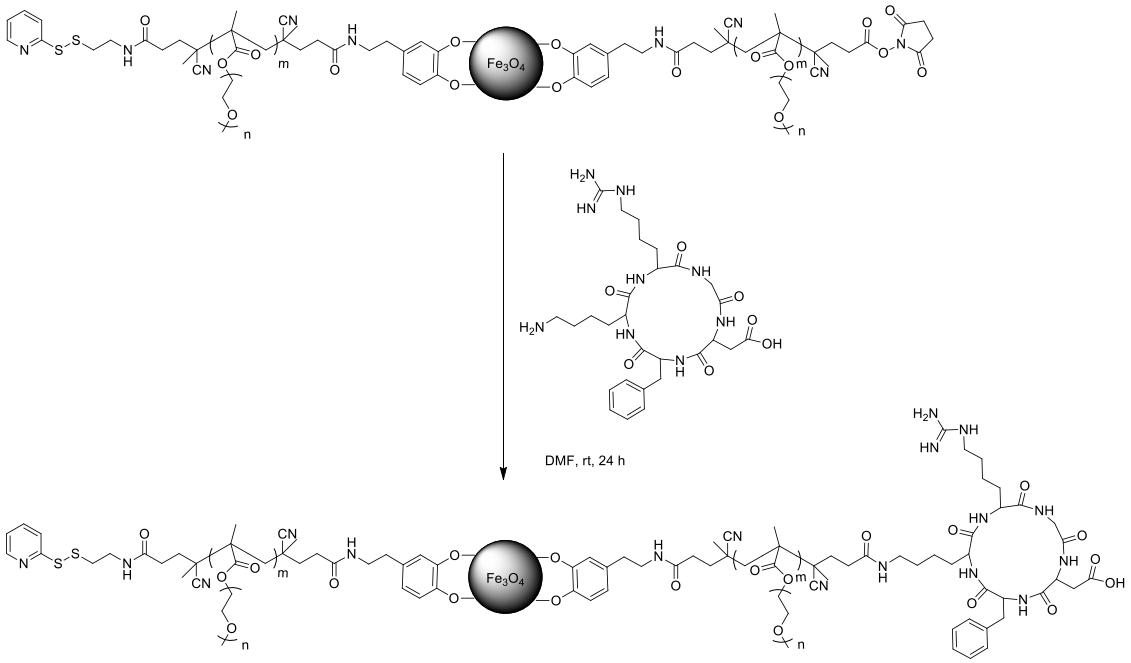

Figure 7.16. Attachment of cRGDfK to Fe_3O_4@PEGMEMA@PDS+NHS nanoparticles.

Characterization of this molecule was achieved by doing BCA assay protocol. After this protocol, the peak at 562 nm in UV spectroscopy proved the presence of cRGDfK attached to the nanoparticles (Figure 7.17). In order to learn how much cRGDfK was attached, a calibration curve was drawn and it was calculated that there are 5 µg of cRGDfK per 1 mg of iron oxide nanoparticles. PDS group existence was confirmed by UV-Vis spectroscopy. The peak at 280 nm shows the existence of the PDS groups (Figure 7.18).

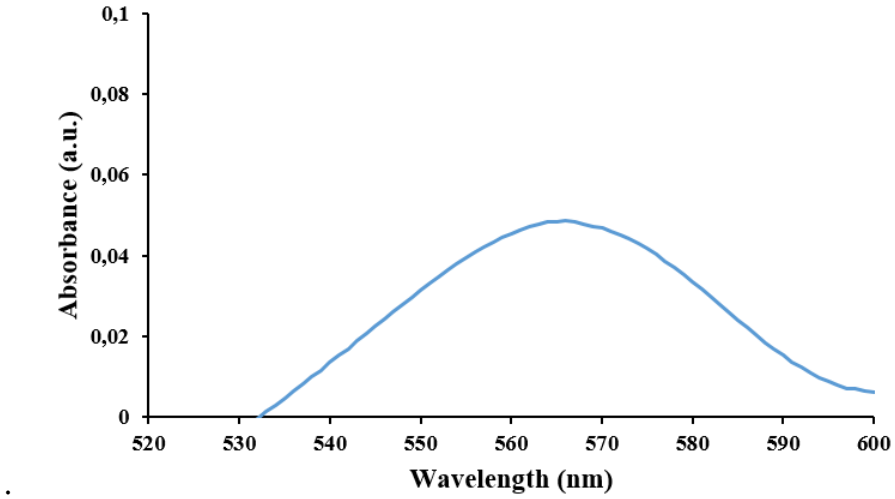

.

Figure 7.17. UV spectroscopy of Fe_3O_4@PEGMEMA@PdS-cRGDfK after BCA Assay protocol.

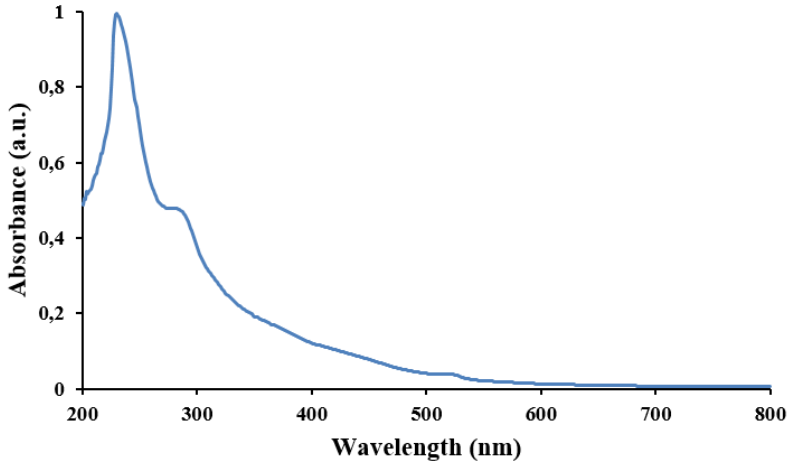

Figure 7.18. UV-Vis Spectroscopy of Fe_3O_4@PEGMEMA@PDS+cRGDfK

After attaching cRGDfK to iron oxide nanoparticles, the remaining NHS groups were reacted with 1-amino-2-propanol to eliminate any side reactions. Because if there were NHS activated carboxylic acid groups in nanoparticles, they would give thio-esterification reaction with thiols, which is not desired for the scope of the project. After the reaction, excess amount of 1-amino-2-propanol was removed by precipitating nanoparticles in diethyl ether. As the future work, thiol bearing anticancer therapeutic agent will be attached since the PDS groups exist there.

8. CONCLUSION

In this project, water dispersible polyethylene glycol based magnetic iron oxide nanoparticles with NHS activated carboxylic acid and pyridyl disulfide functionalized end groups were synthesized by grafting from approach. Oleic acid stabilized iron oxide nanoparticles were synthesized by thermal decomposition method. These magnetic nanoparticles were polymerized with p(PEGMEMA) by RAFT polymerization. The end groups of grafted polymers were trithiocarbonate groups which can be modified with azo initiators. Pyridyl disulfide and NHS activated carboxylic acid containing azo initiators were synthesized. Trithiocarbonate groups of polymer-coated iron oxide nanoparticles were modified using these azo initiators by radical exchange reaction. Pyridyl disulfide groups of these nanoparticles were able to react with a thiol bearing dye molecule to reform reversible disulfide group. NHS activated carboxylic acid groups were able to react with an amine bearing dye to form irreversible amide bond. By using this chemistry, amine bearing cRGDfK targeting group was attached by amide formation. In the future thiol bearing anticancer therapeutic agent will be attached by disulfide formation.

REFERENCES

1. Yigit, M.V., D. Mazumdar, and Y. Lu, “MRI Detection Of Thrombin With Aptamer Functionalized Superparamagnetic Iron Oxide Nanoparticles.”, *Bioconjugate Chemistry*, Vol. 19, pp. 412–417, 2008.

2. Magro, M., D. Baratella, E. Bonaiuto, J. de Almeida Roger, G. Chemello, S. Pasquaroli, L. Mancini, I. Olivotto, G. Zoppellaro, J. Ugolotti, C. Aparicio, A.P. Fifi, G. Cozza, G. Miotto, G. Radaelli, D. Bertotto, R. Zboril, and F. Vianello, “Stealth Iron Oxide Nanoparticles For Organotropic Drug Targeting.”, *Biomacromolecules*, Vol. 20, pp. 1375–1384, 2019.

3. Fuller, E.G., H. Sun, R.D. Dhavalikar, M. Unni, G.M. Scheutz, B.S. Sumerlin, and C. Rinaldi, “Externally Triggered Heat And Drug Release From Magnetically Controlled Nanocarriers.”, *ACS Applied Polymer Materials*, Vol. 1, pp. 211–220, 2019.

4. Albarqi, H.A., L.H. Wong, C. Schumann, F.Y. Sabei, T. Korzun, X. Li, M.N. Hansen, P. Dhagat, A.S. Moses, Olena Taratula, and Oleh Taratula, “Biocompatible Nanoclusters With High Heating Efficiency For Systemically Delivered Magnetic Hyperthermia.”, *ACS Nano*, Vol. 13, pp. 6383–6395, 2019.

5. Schwaminger, S.P., P. Fraga-García, S.A. Blank-Shim, T. Straub, M. Haslbeck, F. Muraca, K.A. Dawson, and S. Berensmeier, “Magnetic One-Step Purification Of His-Tagged Protein By Bare Iron Oxide Nanoparticles.”, *ACS Omega*, Vol. 4, pp. 3790–3799, 2019.

6. Laurent, S., D. Forge, M. Port, A. Roch, C. Robic, L. Vander Elst, and R.N. Muller, “Magnetic Iron Oxide Nanoparticles: Synthesis, Stabilization, Vectorization, Physicochemical Characterizations, And Biological Applications.”, *Chemical Reviews*, Vol. 108, pp. 2064–2110, 2008.

7. Mahmoudi, M., M.A. Sahraian, M.A. Shokrgozar, and S. Laurent, “Superparamagnetic Iron Oxide Nanoparticles: Promises For Diagnosis And Treatment Of Multiple Sclerosis.”, *ACS Chemical Neuroscience*, Vol. 2, pp. 118–140, 2011.

8. Fratila, R.M., S.G. Mitchell, P. del Pino, V. Grazu, and J.M. de la Fuente, “Strategies For The Biofunctionalization Of Gold And Iron Oxide Nanoparticles.”, *Langmuir*, Vol. 30, pp. 15057–15071, 2014.

9. Basiruddin, S., A. Saha, N. Pradhan, and N.R. Jana, “Advances In Coating Chemistry In Deriving Soluble Functional Nanoparticle.”, *The Journal of Physical Chemistry C*, Vol. 114, pp. 11009–11017, 2010.

10. Shubhra, Q.T.H., H. Macková, D. Horák, A. Fodor-Kardos, J. Tóth, J. Gyenis, and T. Feczkó, “Encapsulation Of Human Serum Albumin In Submicrometer Magnetic Poly(Lactide-Co-Glycolide) Particles As A Model System For Targeted Drug Delivery.”, *e-Polymers*, Vol. 13 2013.

11. Mikhaylova, M., D.K. Kim, C.C. Berry, A. Zagorodni, M. Toprak, A.S.G. Curtis, and M. Muhammed, “BSA Immobilization On Amine-Functionalized Superparamagnetic Iron Oxide Nanoparticles.”, *Chemistry of Materials*, Vol. 16, pp. 2344–2354, 2004.

12. Hyeon, T., S.S. Lee, J. Park, Y. Chung, and H. Bin Na, “Synthesis Of Highly Crystalline And Monodisperse Maghemite Nanocrystallites Without A Size-Selection Process.”, *Journal of the American Chemical Society*, Vol. 123, pp. 12798–12801, 2001.

13. Itoh, H., and T. Sugimoto, “Systematic Control Of Size, Shape, Structure, And Magnetic Properties Of Uniform Magnetite And Maghemite Particles.”, *Journal of Colloid and Interface Science*, Vol. 265, pp. 283–295, 2003.

14. Chen, F., Q. Gao, G. Hong, and J. Ni, “Synthesis And Characterization Of Magnetite Dodecahedron Nanostructure By Hydrothermal Method.”, *Journal of Magnetism and Magnetic Materials*, Vol. 320, pp. 1775–1780, 2008.

15. López Pérez, J.A., M.A. López Quintela, J. Mira, J. Rivas, and S.W. Charles, “Advances In The Preparation Of Magnetic Nanoparticles By The Microemulsion Method.”, *The Journal of Physical Chemistry B*, Vol. 101, pp. 8045–8047, 1997.

16. Lee, S.-J., J.-R. Jeong, S.-C. Shin, J.-C. Kim, and J.-D. Kim, “Synthesis And Characterization Of Superparamagnetic Maghemite Nanoparticles Prepared By Coprecipitation Technique.”, *Journal of Magnetism and Magnetic Materials*, Vol. 282, pp. 147–150, 2004.

17. Wu, M.-S., Y.-H. Ou, and Y.-P. Lin, “Iron Oxide Nanosheets And Nanoparticles Synthesized By A Facile Single-Step Coprecipitation Method For Lithium-Ion Batteries.”, *Journal of The Electrochemical Society*, Vol. 158, pp. A231, 2011.

18. Dai, Z., F. Meiser, and H. Möhwald, “Nanoengineering Of Iron Oxide And Iron Oxide/Silica Hollow Spheres By Sequential Layering Combined With A Sol–Gel Process.”, *Journal of Colloid and Interface Science*, Vol. 288, pp. 298–300, 2005.

19. Jensen, K.M.Ø., H.L. Andersen, C. Tyrsted, E.D. Bøjesen, A.-C. Dippel, N. Lock, S.J.L. Billinge, B.B. Iversen, and M. Christensen, “Mechanisms For Iron Oxide Formation Under Hydrothermal Conditions: An In Situ Total Scattering Study.”, *ACS Nano*, Vol. 8, pp. 10704–10714, 2014.

20. Cai, H., X. An, J. Cui, J. Li, S. Wen, K. Li, M. Shen, L. Zheng, G. Zhang, and X. Shi, “Facile Hydrothermal Synthesis And Surface Functionalization Of Polyethyleneimine-Coated Iron Oxide Nanoparticles For Biomedical Applications.”, *ACS Applied Materials & Interfaces*, Vol. 5, pp. 1722–1731, 2013.

21. Housaindokht, M.R., and A. Nakhaei Pour, “Size Control Of Iron Oxide Nanoparticles Using Reverse Microemulsion Method: Morphology, Reduction, And Catalytic Activity In CO Hydrogenation.”, *Journal of Chemistry*, Vol. 2013, pp. 1–10, 2013.

22. Park, J., K. An, Y. Hwang, J.-G. Park, H.-J. Noh, J.-Y. Kim, J.-H. Park, N.-M. Hwang, and T. Hyeon, “Ultra-Large-Scale Syntheses Of Monodisperse Nanocrystals.”, *Nature Materials*, Vol. 3, pp. 891–895, 2004.

23. Lu, A.-H., E.L. Salabas, and F. Schüth, “Magnetic Nanoparticles: Synthesis, Protection, Functionalization, And Application.”, *Angewandte Chemie International Edition*, Vol. 46, pp. 1222–1244, 2007.

24. Roca, A.G., M.P. Morales, and C.J. Serna, “Synthesis Of Monodispersed Magnetite Particles From Different Organometallic Precursors.”, *IEEE Transactions on Magnetics*, Vol. 42, pp. 3025–3029, 2006.

25. Ozel, F., H. Kockar, S. Beyaz, O. Karaagac, and T. Tanrisever, “Superparamagnetic Iron Oxide Nanoparticles: Effect Of Iron Oleate Precursors Obtained With A Simple Way.”, *Journal of Materials Science: Materials in Electronics*, Vol. 24, pp. 3073–3080, 2013.

26. Wu, L., A. Mendoza-Garcia, Q. Li, and S. Sun, “Organic Phase Syntheses Of Magnetic Nanoparticles And Their Applications.”, *Chemical Reviews*, Vol. 116, pp. 10473–10512, 2016.

27. Jana, N.R., Y. Chen, and X. Peng, “Size- And Shape-Controlled Magnetic (Cr, Mn, Fe, Co, Ni) Oxide Nanocrystals Via A Simple And General Approach.”, *Chemistry of Materials*, Vol. 16, pp. 3931–3935, 2004.

28. Ling, D., N. Lee, and T. Hyeon, “Chemical Synthesis and Assembly Of Uniformly Sized Iron Oxide Nanoparticles For Medical Applications.”, *Accounts of Chemical Research*, Vol. 48, pp. 1276–1285, 2015.

29. Hyeon, T., “Chemical Synthesis Of Magnetic Nanoparticles.”, *Chemical Communications*, pp. 927–934, 2003.

30. Wu, N., L. Fu, M. Su, M. Aslam, K.C. Wong, and V.P. Dravid, “Interaction Of Fatty Acid Monolayers With Cobalt Nanoparticles.”, *Nano Letters*, Vol. 4, pp. 383–386, 2004.

31. Chan, N., M. Laprise-Pelletier, P. Chevallier, A. Bianchi, M.-A. Fortin, and J.K. Oh, “Multidentate Block-Copolymer-Stabilized Ultrasmall Superparamagnetic Iron Oxide Nanoparticles With Enhanced Colloidal Stability For Magnetic Resonance Imaging.”, *Biomacromolecules*, Vol. 15, pp. 2146–2156, 2014.

32. Lu, C., L.R. Bhatt, H.Y. Jun, S.H. Park, and K.Y. Chai, “Carboxyl–Polyethylene Glycol–Phosphoric Acid: A Ligand For Highly Stabilized Iron Oxide Nanoparticles.”, *Journal of Materials Chemistry*, Vol. 22, pp. 19806, 2012.

33. Das, M., D. Bandyopadhyay, R.P. Singh, H. Harde, S. Kumar, and S. Jain, “Orthogonal Biofunctionalization Of Magnetic Nanoparticles Via ‘Clickable’ Poly(Ethylene Glycol) Silanes: A ‘Universal Ligand’ Strategy To Design Stealth And Target-Specific Nanocarriers.”, *Journal of Materials Chemistry*, Vol. 22, pp. 24652, 2012.

34. Na, H. Bin, G. Palui, J.T. Rosenberg, X. Ji, S.C. Grant, and H. Mattoussi, “Multidentate Catechol-Based Polyethylene Glycol Oligomers Provide Enhanced Stability And Biocompatibility To Iron Oxide Nanoparticles.”, *ACS Nano*, Vol. 6, pp. 389–399, 2012.

35. Chen, L.X., T. Liu, M.C. Thurnauer, R. Csencsits, and T. Rajh, “Fe 2 O 3 Nanoparticle Structures Investigated By X-Ray Absorption Near-Edge Structure, Surface Modifications, And Model Calculations.”, *The Journal of Physical Chemistry B*, Vol. 106, pp. 8539–8546, 2002.

36. Rajh, T., M.C. Thurnauer, P. Thiyagarajan, and M. Tiede, “Structural Characterization Of Self-Organized TiO 2 Nanoclusters Studied By Small Angle Neutron Scattering.”, *The Journal of Physical Chemistry B*, Vol. 103, pp. 2172–2177, 1999.

37. Stone, R.C., B. Qi, D. Trebatoski, R. Jetti, Y.P. Bandera, H. Foulger, and O.T. Mefford, “A Versatile Stable Platform For Multifunctional Applications: Synthesis Of A NitroDOPA–PEO–Alkyne Scaffold For Iron Oxide Nanoparticles.”, *J. Mater. Chem. B*, Vol. 2, pp. 4789–4793, 2014.

38. Groult, H., I. García-Álvarez, L. Romero-Ramírez, M. Nieto-Sampedro, F. Herranz, A. Fernández-Mayoralas, and J. Ruiz-Cabello, “Micellar Iron Oxide Nanoparticles Coated With Anti-Tumor Glycosides.”, *Nanomaterials*, Vol. 8, pp. 567, 2018.

39. Dai, F., M. Du, Y. Liu, G. Liu, Q. Liu, and X. Zhang, “Folic Acid-Conjugated Glucose And Dextran Coated Iron Oxide Nanoparticles As MRI Contrast Agents For Diagnosis And Treatment Response Of Rheumatoid Arthritis.”, *J. Mater. Chem. B*, Vol. 2, pp. 2240–2247, 2014.

40. Kim, D.K., M. Mikhaylova, F.H. Wang, J. Kehr, B. Bjelke, Y. Zhang, T. Tsakalakos, and M. Muhammed, “Starch-Coated Superparamagnetic Nanoparticles As MR Contrast Agents.”, *Chemistry of Materials*, Vol. 15, pp. 4343–4351, 2003.

41. Olsen, D., “Recombinant Collagen And Gelatin For Drug Delivery.”, *Advanced Drug Delivery Reviews*, Vol. 55, pp. 1547–1567, 2003.

42. Li, G., K. Huang, Y. Jiang, P. Ding, and D. Yang, “Preparation And Characterization Of Carboxyl Functionalization Of Chitosan Derivative Magnetic Nanoparticles.”, *Biochemical Engineering Journal*, Vol. 40, pp. 408–414, 2008.

43. Mondini, S., S. Cenedese, G. Marinoni, G. Molteni, N. Santo, C.L. Bianchi, and A. Ponti, “One-Step Synthesis And Functionalization Of Hydroxyl-Decorated Magnetite Nanoparticles.”, *Journal of Colloid and Interface Science*, Vol. 322, pp. 173–179, 2008.

44. Mahmoudi, M., A. Simchi, and M. Imani, “Cytotoxicity Of Uncoated And Polyvinyl Alcohol Coated Superparamagnetic Iron Oxide Nanoparticles.”, *The Journal of Physical Chemistry C*, Vol. 113, pp. 9573–9580, 2009.

45. Chen, F., Q. Gao, G. Hong, and J. Ni, “Synthesis Of Magnetite Core–Shell Nanoparticles By Surface-Initiated Ring-Opening Polymerization Of L-Lactide.”, *Journal of Magnetism and Magnetic Materials*, Vol. 320, pp. 1921–1927, 2008.

46. Singh, H., P.E. Laibinis, and T.A. Hatton, “Rigid, Superparamagnetic Chains Of Permanently Linked Beads Coated With Magnetic Nanoparticles. Synthesis And Rotational Dynamics Under Applied Magnetic Fields.”, *Langmuir*, Vol. 21, pp. 11500–11509, 2005.

47. Shan, G., J. Xing, M. Luo, H. Liu, and J. Chen, “Immobilization Of Pseudomonas Delafieldii With Magnetic Polyvinyl Alcohol Beads And Its Application In Biodesulfurization.”, *Biotechnology Letters*, Vol. 25, pp. 1977–1981, 2003.

48. Sandiford, L., A. Phinikaridou, A. Protti, L.K. Meszaros, X. Cui, Y. Yan, G. Frodsham, P.A. Williamson, N. Gaddum, R.M. Botnar, P.J. Blower, M.A. Green, and R.T.M. de Rosales, “Bisphosphonate-Anchored PEGylation And Radiolabeling Of Superparamagnetic Iron Oxide: Long-Circulating Nanoparticles For In Vivo Multimodal (T1 MRI-SPECT) Imaging.”, *ACS Nano*, Vol. 7, pp. 500–512, 2013.

49. Larsen, E.K.U., T. Nielsen, T. Wittenborn, H. Birkedal, T. Vorup-Jensen, M.H. Jakobsen, L. Østergaard, M.R. Horsman, F. Besenbacher, K.A. Howard, and J. Kjems, “Size-Dependent Accumulation Of PEGylated Silane-Coated Magnetic Iron Oxide Nanoparticles In Murine Tumors.”, *ACS Nano*, Vol. 3, pp. 1947–1951, 2009.

50. Torrisi, V., A. Graillot, L. Vitorazi, Q. Crouzet, G. Marletta, C. Loubat, and J.-F. Berret, “Preventing Corona Effects: Multiphosphonic Acid Poly(Ethylene Glycol) Copolymers For Stable Stealth Iron Oxide Nanoparticles.”, *Biomacromolecules*, Vol. 15, pp. 3171–3179, 2014.

51. Biggs, C.I., M. Walker, and M.I. Gibson, “‘Grafting To’ Of RAFTed Responsive Polymers To Glass Substrates By Thiol–Ene And Critical Comparison To Thiol–Gold Coupling.”, *Biomacromolecules*, Vol. 17, pp. 2626–2633, 2016.

52. Choi, W.S., J.-H. Park, H.Y. Koo, J.-Y. Kim, B.K. Cho, and D.-Y. Kim, “Grafting-From

Polymerization Inside A Polyelectrolyte Hollow-Capsule Microreactor.", *Angewandte Chemie International Edition*, Vol. 44, pp. 1096–1101, 2005.

53. Scales, C.W., A.J. Convertine, and C.L. McCormick, "Fluorescent Labeling Of RAFT-Generated Poly(N -Isopropylacrylamide) Via A Facile Maleimide−Thiol Coupling Reaction †.", *Biomacromolecules*, Vol. 7, pp. 1389–1392, 2006.

54. Yeole, N., "Thiocarbonylthio Compounds.", *Synlett*, Vol. 2010, pp. 1572–1573, 2010.

55. Moad, G., "RAFT Polymerization – Then And Now.", pp. 211–246, 2015.

56. Moad, G., R.T.A. Mayadunne, E. Rizzardo, M. Skidmore, and S.H. Thang, "Kinetics And Mechanism Of RAFT Polymerization.", pp. 520–535, 2003.

57. Boyer, C., V. Bulmus, J. Liu, T.P. Davis, M.H. Stenzel, and C. Barner-Kowollik, "Well-Defined Protein−Polymer Conjugates Via I N Situ RAFT Polymerization.", *Journal of the American Chemical Society*, Vol. 129, pp. 7145–7154, 2007.

58. Kim, B.J., S. Given-Beck, J. Bang, C.J. Hawker, and E.J. Kramer, "Importance Of End-Group Structure In Controlling The Interfacial Activity Of Polymer-Coated Nanoparticles.", *Macromolecules*, Vol. 40, pp. 1796–1798, 2007.

59. Oz, Y., M. Arslan, T.N. Gevrek, R. Sanyal, and A. Sanyal, "Modular Fabrication Of Polymer Brush Coated Magnetic Nanoparticles: Engineering The Interface For Targeted Cellular Imaging.", *ACS Applied Materials & Interfaces*, Vol. 8, pp. 19813–19826, 2016.

60. Anderson, G.W., J.E. Zimmerman, and F.M. Callahan, "N-Hydroxysuccinimide Esters In Peptide Synthesis.", *Journal of the American Chemical Society*, Vol. 85, pp. 3039–3039, 1963.

61. Radzicka, A., and R. Wolfenden, "Rates Of Uncatalyzed Peptide Bond Hydrolysis In Neutral Solution And The Transition State Affinities Of Proteases.", *Journal of the American Chemical Society*, Vol. 118, pp. 6105–6109, 1996.

62. Gok, O., P. Erturk, B. Sumer Bolu, T.N. Gevrek, R. Sanyal, and A. Sanyal, "Dendrons And Multiarm Polymers With Thiol-Exchangeable Cores: A Reversible Conjugation Platform For Delivery.", *Biomacromolecules*, Vol. 18, pp. 2463–2477, 2017.

63. Tang, R., J. Xue, B. Xu, D. Shen, G.P. Sudlow, and S. Achilefu, “Tunable Ultrasmall Visible-To-Extended Near-Infrared Emitting Silver Sulfide Quantum Dots For Integrin-Targeted Cancer Imaging.”, *ACS Nano*, Vol. 9, pp. 220–230, 2015.

64. Fava, A., A. Iliceto, and E. Camera, “Kinetics Of The Thiol-Disulfide Exchange.”, *Journal of the American Chemical Society*, Vol. 79, pp. 833–838, 1957.

65. Kerr, J., J.L. Schlosser, D.R. Griffin, D.Y. Wong, and A.M. Kasko, “Steric Effects In Peptide And Protein Exchange With Activated Disulfides.”, *Biomacromolecules*, Vol. 14, pp. 2822–2829, 2013.

66. Balendiran, G.K., R. Dabur, and D. Fraser, “The Role Of Glutathione In Cancer.”, *Cell Biochemistry and Function*, Vol. 22, pp. 343–352, 2004.

67. Xu, Z., S. Liu, Y. Kang, and M. Wang, “Glutathione-Responsive Polymeric Micelles Formed By A Biodegradable Amphiphilic Triblock Copolymer For Anticancer Drug Delivery And Controlled Release.”, *ACS Biomaterials Science & Engineering*, Vol. 1, pp. 585–592, 2015.

68. Aktan, B., L. Chambre, R. Sanyal, and A. Sanyal, “‘Clickable’ Nanogels Via Thermally Driven Self-Assembly Of Polymers: Facile Access To Targeted Imaging Platforms Using Thiol–Maleimide Conjugation.”, *Biomacromolecules*, Vol. 18, pp. 490–497, 2017.

69. Ruan, Z., P. Yuan, T. Li, Y. Tian, Q. Cheng, and L. Yan, “Glutathione Triggered Near Infrared Fluorescence Imaging-Guided Chemotherapy By Cyanine Conjugated Polypeptide.”, *ACS Biomaterials Science & Engineering*, Vol. 4, pp. 4208–4218, 2018.

70. Oyeneye, O.O., W. Xu, and P.A. Charpentier, “Adhesive RAFT Agents For Controlled Polymerization Of Acrylamide: Effect Of Catechol-End R Groups.”, *RSC Advances*, Vol. 5, pp. 76919–76926, 2015.

71. Saha, B., U. Haldar, and P. De, “Polymer-Chlorambucil Drug Conjugates: A Dynamic Platform Of Anticancer Drug Delivery.”, *Macromolecular Rapid Communications*, Vol. 37, pp. 1015–1020, 2016.

72. Wang, H., Z. Chen, L. Xin, J. Cui, S. Zhao, and Y. Yan, “Synthesis Of Pyrene-Capped Polystyrene By Free Radical Polymerization And Its Application In Direct Exfoliation

Of Graphite Into Graphene Nanosheets.", *Journal of Polymer Science Part A: Polymer Chemistry*, Vol. 53, pp. 2175–2185, 2015.

73. Lee, S.H., J.Y. Lee, J.S. Kim, T.G. Park, and H. Mok, "Amphiphilic SiRNA Conjugates For Co-Delivery Of Nucleic Acids And Hydrophobic Drugs.", *Bioconjugate Chemistry*, Vol. 28, pp. 2051–2061, 2017.

74. Etrych, T., L. Kovář, V. Šubr, A. Braunová, M. Pechar, P. Chytil, B. Říhova, and K. Ulbrich, "High-Molecular-Weight Polymers Containing Biodegradable Disulfide Bonds: Synthesis And In Vitro Verification Of Intracellular Degradation.", *Journal of Bioactive and Compatible Polymers*, Vol. 25, pp. 5–26, 2010.

APPENDIX A: COPYRIGHT NOTICES

Coppyrights that belong to figures and chapters which were taken from literature articles can be found here.

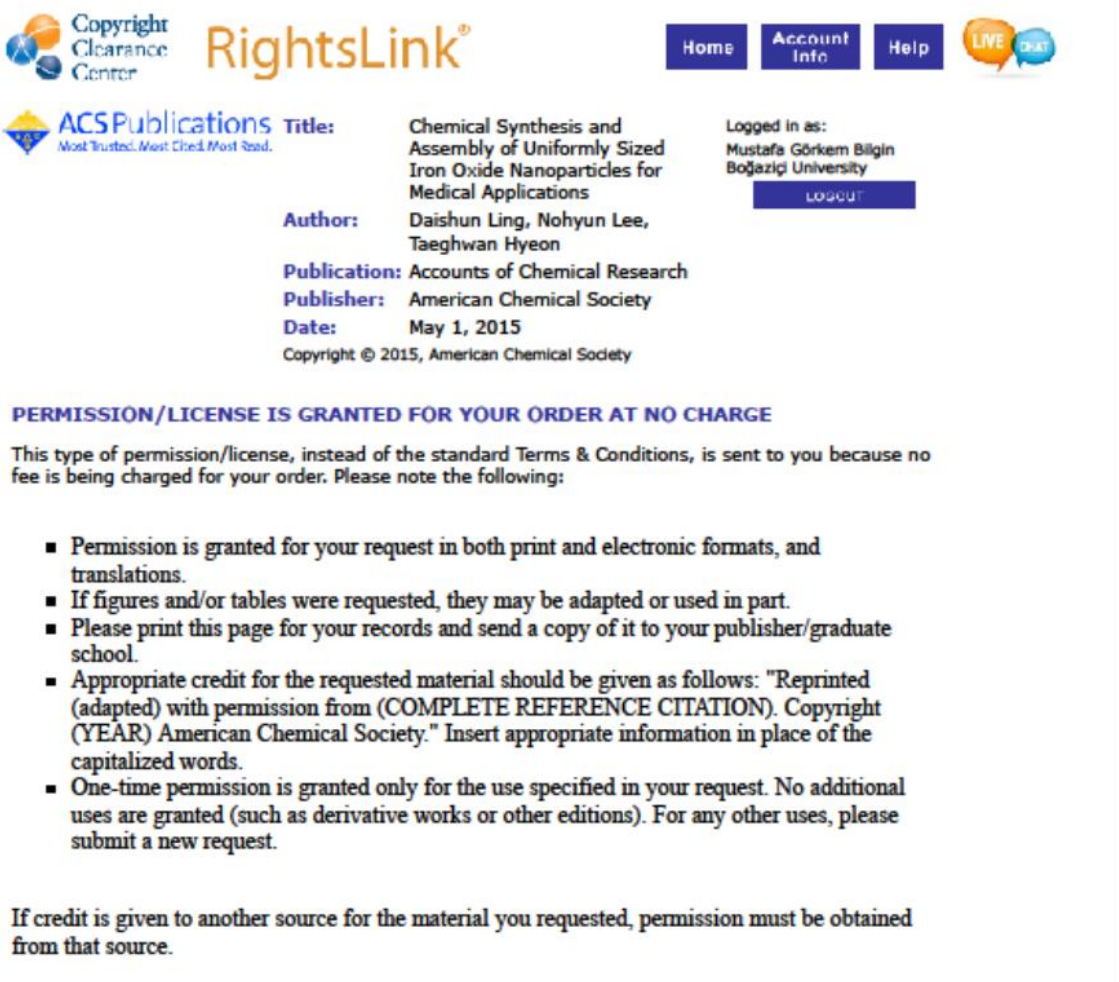

Copyright Clearance Center RightsLink®

Home | Account Info | Help | LIVE CHAT

ACS Publications Most Trusted. Most Cited. Most Read.

Title: Chemical Synthesis and Assembly of Uniformly Sized Iron Oxide Nanoparticles for Medical Applications

Author: Daishun Ling, Nohyun Lee, Taeghwan Hyeon

Publication: Accounts of Chemical Research

Publisher: American Chemical Society

Date: May 1, 2015

Copyright © 2015, American Chemical Society

Logged in as:
Mustafa Görkem Bilgin
Boğaziçi University
LOGOUT

PERMISSION/LICENSE IS GRANTED FOR YOUR ORDER AT NO CHARGE

This type of permission/license, instead of the standard Terms & Conditions, is sent to you because no fee is being charged for your order. Please note the following:

- Permission is granted for your request in both print and electronic formats, and translations.
- If figures and/or tables were requested, they may be adapted or used in part.
- Please print this page for your records and send a copy of it to your publisher/graduate school.
- Appropriate credit for the requested material should be given as follows: "Reprinted (adapted) with permission from (COMPLETE REFERENCE CITATION). Copyright (YEAR) American Chemical Society." Insert appropriate information in place of the capitalized words.
- One-time permission is granted only for the use specified in your request. No additional uses are granted (such as derivative works or other editions). For any other uses, please submit a new request.

If credit is given to another source for the material you requested, permission must be obtained from that source.

Figure A.1. Copyright license of [28]

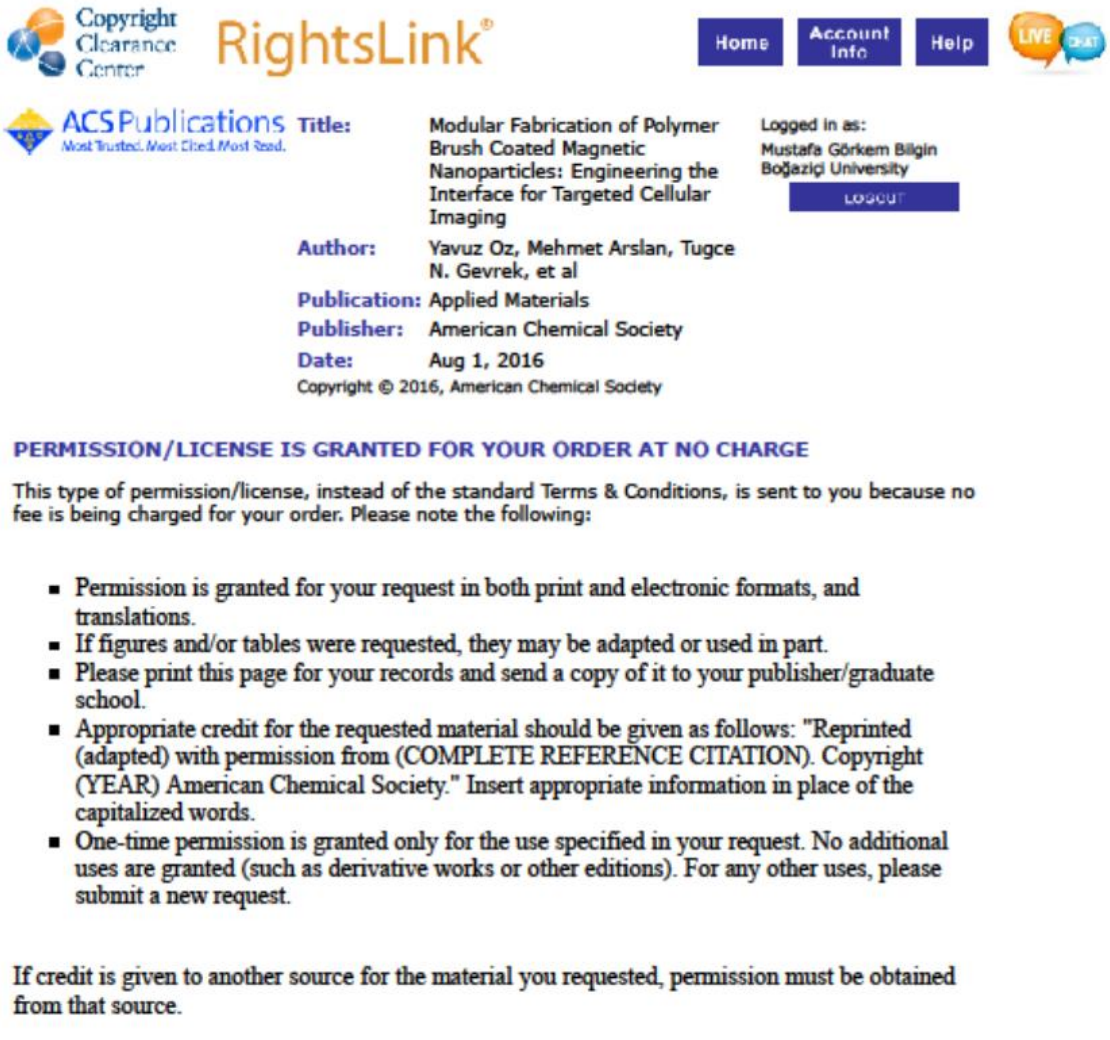

Copyright Clearance Center RightsLink®

Home | Account Info | Help | LIVE CHAT

ACS Publications
Most Trusted. Most Cited. Most Read.

Title: Modular Fabrication of Polymer Brush Coated Magnetic Nanoparticles: Engineering the Interface for Targeted Cellular Imaging

Author: Yavuz Oz, Mehmet Arslan, Tugce N. Gevrek, et al

Publication: Applied Materials

Publisher: American Chemical Society

Date: Aug 1, 2016

Copyright © 2016, American Chemical Society

Logged in as:
Mustafa Görkem Bilgin
Boğaziçi University
LOGOUT

PERMISSION/LICENSE IS GRANTED FOR YOUR ORDER AT NO CHARGE

This type of permission/license, instead of the standard Terms & Conditions, is sent to you because no fee is being charged for your order. Please note the following:

- Permission is granted for your request in both print and electronic formats, and translations.
- If figures and/or tables were requested, they may be adapted or used in part.
- Please print this page for your records and send a copy of it to your publisher/graduate school.
- Appropriate credit for the requested material should be given as follows: "Reprinted (adapted) with permission from (COMPLETE REFERENCE CITATION). Copyright (YEAR) American Chemical Society." Insert appropriate information in place of the capitalized words.
- One-time permission is granted only for the use specified in your request. No additional uses are granted (such as derivative works or other editions). For any other uses, please submit a new request.

If credit is given to another source for the material you requested, permission must be obtained from that source.

Figure A.2. Copyright license of [59]

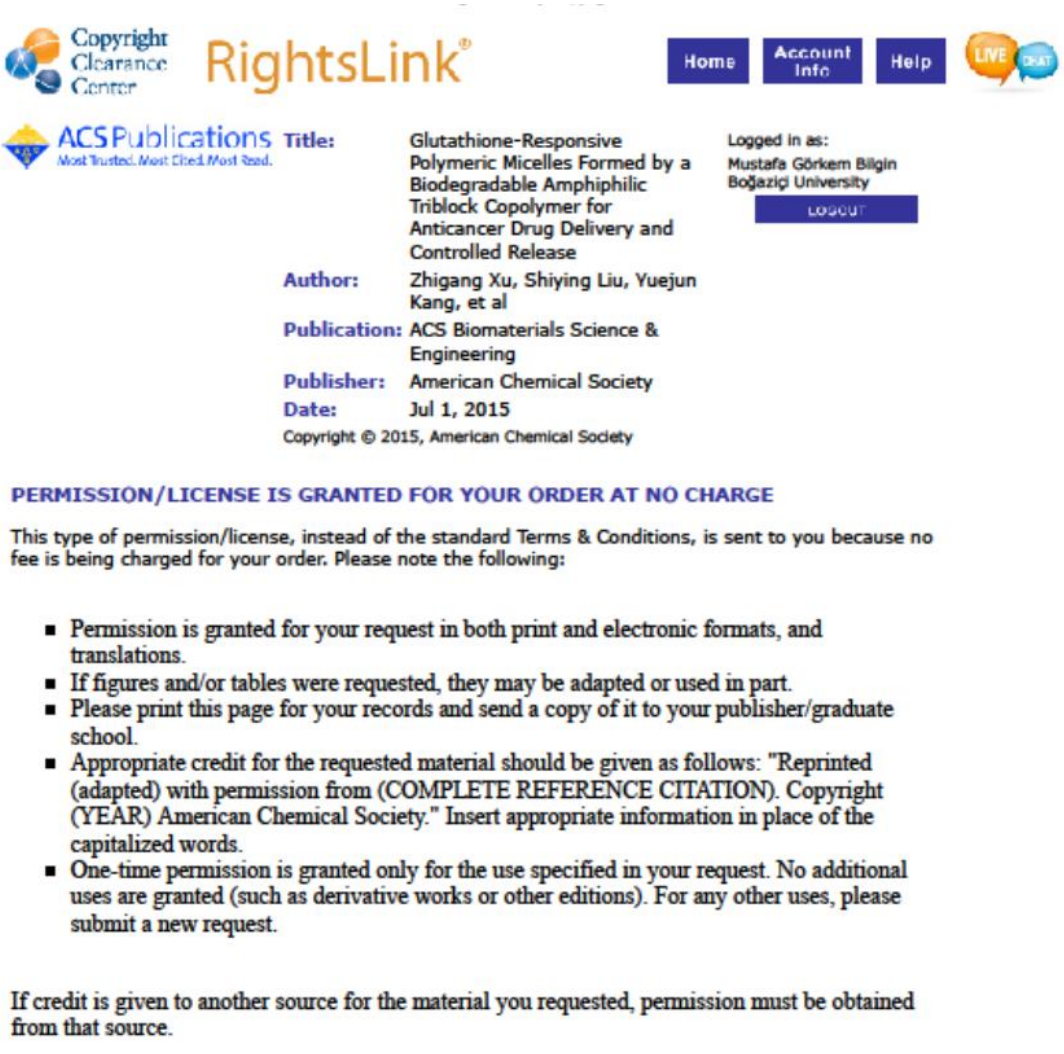

Copyright Clearance Center RightsLink®

Home | Account Info | Help | LIVE CHAT

ACS Publications
Most Trusted. Most Cited. Most Read.

Title: Glutathione-Responsive Polymeric Micelles Formed by a Biodegradable Amphiphilic Triblock Copolymer for Anticancer Drug Delivery and Controlled Release

Author: Zhigang Xu, Shiying Liu, Yuejun Kang, et al

Publication: ACS Biomaterials Science & Engineering

Publisher: American Chemical Society

Date: Jul 1, 2015

Copyright © 2015, American Chemical Society

Logged in as:
Mustafa Görkem Bilgin
Boğaziçi University
LOGOUT

PERMISSION/LICENSE IS GRANTED FOR YOUR ORDER AT NO CHARGE

This type of permission/license, instead of the standard Terms & Conditions, is sent to you because no fee is being charged for your order. Please note the following:

- Permission is granted for your request in both print and electronic formats, and translations.
- If figures and/or tables were requested, they may be adapted or used in part.
- Please print this page for your records and send a copy of it to your publisher/graduate school.
- Appropriate credit for the requested material should be given as follows: "Reprinted (adapted) with permission from (COMPLETE REFERENCE CITATION). Copyright (YEAR) American Chemical Society." Insert appropriate information in place of the capitalized words.
- One-time permission is granted only for the use specified in your request. No additional uses are granted (such as derivative works or other editions). For any other uses, please submit a new request.

If credit is given to another source for the material you requested, permission must be obtained from that source.

Figure A.3. Copyright license of [67]